
Classification of Superstatistical Features in High Dimensions

Urte Adomaityte
Department of Mathematics
King's College London
urte.adomaityte@kcl.ac.uk

Gabriele Sicuro
Department of Mathematics
King's College London
gabriele.sicuro@kcl.ac.uk

Pierpaolo Vivo
Department of Mathematics
King's College London
pierpaolo.vivo@kcl.ac.uk

Abstract

We characterise the learning of a mixture of two clouds of data points with generic centroids via empirical risk minimisation in the high dimensional regime, under the assumptions of generic convex loss and convex regularisation. Each cloud of data points is obtained by sampling from a possibly uncountable superposition of Gaussian distributions, whose variance has a generic probability density ϱ . Our analysis covers therefore a large family of data distributions, including the case of power-law-tailed distributions with no covariance. We study the generalisation performance of the obtained estimator, we analyse the role of regularisation, and the dependence of the separability transition on the distribution scale parameters.

1 Introduction

Despite their simplicity, generalised linear models (GLMs) are still ubiquitous in the theoretical research on machine learning. Their nontrivial phenomenology is indeed often amenable to complete analytical treatment and has been a powerful key to understanding the unexpected behavior of large and complex architectures. Random features models [47, 35, 18], for example, allowed to clarify many aspects of the well-known double-descent phenomenon in neural networks [41, 5, 6]. Over the years, a variety of GLMs has been proposed to investigate a number of aspects of the problem of learning in high dimension, with a line of research that spans more than three decades [51, 55]. Yet, a crucial assumption adopted in many such theoretical models is that the covariates are obtained from a *Gaussian* distribution, or from a mixture of Gaussian distributions [30, 37, 2, 25, 31]. Such Gaussian design has served as a convenient working hypothesis that, in some cases, can be experimentally and theoretically justified [50, 32]. It is however not obvious how much such a theoretical assumption limits the scope of the obtained insights: it is reasonable to expect structure, fat tails, and large fluctuations in real (often non-Gaussian) data [1, 48] to play an important role in the learning process, and it would be therefore desirable to include structured and heavy-tailed-distributed covariates in our theoretical toolbox.

This paper presents, to the best of our knowledge for the first time, the exact asymptotics for classification tasks on covariates obtained from a mixture of heavy-tailed distributions. We will focus on supervised binary classification assuming that the sample size n and the dimensionality d of the space where the covariates live are both sent to infinity, keeping their ratio $n/d = \alpha$ fixed. The paper fits therefore in the line of works on exact high-dimensional asymptotics for classification learning via a GLM [37, 31], but, crucially, we relax the usual Gaussian hypothesis by including in

our analysis power-law-tailed distributions with possibly no covariance. The mixture is obtained from two distributions, each resulting from a *possibly uncountable* superposition of Gaussian distributions with covariance $\Sigma = \Delta \mathbf{I}_d \in \mathbb{R}^{d \times d}$ to be intended itself as a random variable, so that Δ has density ϱ . Using, for example, an appropriately parametrised inverse-Gamma distribution for ϱ , such a *superstatistical* construction [3, 4] provides a fat-tailed, Cauchy-like data distribution with infinite covariance. The replica method [36], an analytical tool widely adopted in statistical physics, provides asymptotic formulas for a generic density ϱ , allowing us to study the effects of non-Gaussianity on the performance curves, and test Gaussian universality hypotheses [46] in such a classification task.

Motivation and related works Learning a rule to classify data points clustered in clouds in high dimension is a classical problem in statistics [22]. Its ubiquity is exemplified by the recently observed neural collapse phenomenon in deep neural networks, in which the last layer classifier is found to operate on features clustered in clouds around the vertices of a simplex [26, 43]; more recently, Seddik et al. [50] showed that Gaussian mixtures suitably describe the deep learning representation of GAN data. In theoretical models, data points are typically assumed to be organised in K *Gaussian* clouds, each corresponding to a class. Each class k , $k \in \{1, \dots, K\}$, is centered around a mean vector μ_k and has covariance Σ_k . The binary classification case, $K = 2$, is the simplest, and possibly most studied, setting. Mai and Liao [34] considered an ERM task with generic convex loss and ridge regularisation in the high-dimensional regime $n, d \rightarrow +\infty$ with $n/d \in (0, +\infty)$. In this setting, they gave a precise prediction of the classification error, showing the optimality of the square loss in the unregularised case. Their results have been extended by Mignacco et al. [37], who showed that the presence of a regularisation can actually drastically affect the performance, improving it. In the same setting, the Bayes optimal estimator has been studied in both the supervised and the semi-supervised setting [37, 29]. Almost-Bayes-optimal solutions have been put in relation to wide flat landscape regions [2]. In the context of binary classification, the maximum number n of samples that can be perfectly fitted by a linear model in dimension d [37, 12, 25] has been the topic of investigation since the seminal work of Cover [8] and is related to the classical storage capacity problems on networks [15, 16, 27]. The corresponding separability threshold value $\alpha = n/d$ is remarkably associated with the existence transition of the maximum likelihood estimator [53, 57]. The precise asymptotic characterisation of the test error in learning to classify $K \geq 2$ Gaussian clouds with generic means and covariances has been recently obtained by Loureiro et al. [31].

As mentioned previously, the working hypothesis of *Gaussian design* is widely adopted in high-dimensional classification problems. On top of being a convenient theoretical hypothesis, this assumption has been justified in terms of a “Gaussian universality” principle. In other words, in a number of circumstances, non-Gaussian distributions are found to be effectively described by Gaussian ones with matching first and second moments as far as the asymptotic properties of the estimators are concerned [32]. Such a “universality property” has been rigorously proven for example in compressed sensing [38] or in the case of LASSO with non-Gaussian dictionaries [42]. A Gaussian equivalence principle introduced by Goldt et al. [20] has been proven to hold for a wide class of generalised linear estimation problems [35]. Extending a work by Hu and Lu [24], Montanari and Saeed [39] recently proved such a principle in a GLM under the assumption of pointwise normality of the distribution of the features. This crucial assumption can be intended, roughly speaking, as the assumption of sub-Gaussian decay of a marginal of the feature distribution in any direction (see also [17, 9] for further developments).

The Gaussian universality principle, however, can break down by relaxing some of the aforementioned assumptions on the feature distribution. Montanari and Saeed [39] for example showed that pointwise normality is a *necessary* hypothesis for universality. Studying elliptic regression tasks on elliptical distribution, El Karoui [13] made evident that the statistics of the estimator can depend on higher moments of the dataset distribution [13, 52, 54]. More recently, Pesce et al. [46] showed that a structured Gaussian mixture cannot be effectively described by a single Gaussian cloud. Building upon a series of contributions related to the asymptotic performance of models in the proportional high-dimensional limit [23, 35, 19, 18, 21, 32], we aim precisely to explore the validity of Gaussian universality within classification problems. In our work, we adopt the aforementioned “superstatistical setting” [3, 4] by considering a very large family of non-Gaussian distributions, including the case of power-law-tailed distributions with infinite covariance.

Our contributions In this manuscript we provide the following results.

- We study a classification task on a non-Gaussian mixture model in Eq. (1) below and we analytically derive, using the replica method [10, 14, 36], an asymptotic characterisation of the statistics of the empirical risk minimisation (ERM) estimator. Our results go beyond the usual Gaussian assumption and include for example the case of covariates from a mixture of distributions with infinite variance. The analysis is performed in the high-dimensional, proportional limit and for any convex loss and convex regularisation. By using this result, we provide asymptotic formulas for the generalisation, training errors and training loss.
- We analyse the performance of such ERM task on a specific family of point distributions by using different convex loss functions (quadratic and logistic) and ridge regularisation. We show in particular that, in the case of two balanced clusters with a specific non-Gaussian distribution, the optimal ridge regularisation strength λ^* is finite, at odds with the Gaussian case, for which $\lambda^* \rightarrow \infty$ [37].
- We estimate the separability threshold on a large family of data point distributions, including the case of infinite-variance clouds, comparing our results to the known asymptotics for Gaussian clouds [37]. The result of Cover [8] is recovered in the case of infinite distribution width.
- We finally extend recent results on Gaussian universality in the Gaussian mixture model with random labels [17, 46] to the case of non-Gaussian distributions with possibly infinite covariance. We show that the universal formula for the square training loss at zero regularisation found in [17] holds in this more general setting as well.

2 Main result

Dataset construction We consider the task of classifying two data clusters in the d -dimensional space \mathbb{R}^d . The dataset $\mathcal{D} := \{(\mathbf{x}^y, y^y)\}_{y \in [n]}$ is obtained by extracting n independent datapoints \mathbf{x}^y , each associated with a label $y^y \in \{-1, 1\}$. The point positions are correlated with the labels via a law $P(\mathbf{x}, y)$ which we assume to have the form

$$P(\mathbf{x}, y) = \delta_{y,1} \rho P(\mathbf{x}|\boldsymbol{\mu}_+) + \delta_{y,-1} (1 - \rho) P(\mathbf{x}|\boldsymbol{\mu}_-), \quad \rho \in (0, 1), \quad \boldsymbol{\mu}_\pm \in \mathbb{R}^d. \quad (1a)$$

Here $P(\mathbf{x}|\boldsymbol{\mu})$ is a distribution with mean $\boldsymbol{\mu}$, and the mean vectors $\boldsymbol{\mu}_\pm \in \mathbb{R}^d$ are distributed according to some density, such that $\mathbb{E}[\|\boldsymbol{\mu}\|^2] = \Theta(1)$, and correspond to the center of the two clusters. The scalar quantity ρ weighs the relative contribution of the two clusters: in the following, we will denote $\rho_+ = \rho = 1 - \rho_-$. Each cluster distribution $P(\mathbf{x}|\boldsymbol{\mu})$ around a vector $\boldsymbol{\mu}$ is assumed to have the form

$$P(\mathbf{x}|\boldsymbol{\mu}) := \mathbb{E}_\Delta [\mathcal{N}(\mathbf{x}|\boldsymbol{\mu}, \Delta \mathbf{I}_d)], \quad (1b)$$

where $\mathcal{N}(\mathbf{x}|\boldsymbol{\mu}, \boldsymbol{\Sigma})$ is a Gaussian distribution with mean $\boldsymbol{\mu} \in \mathbb{R}^d$ and covariance $\boldsymbol{\Sigma} \in \mathbb{R}^{d \times d}$, and Δ is randomly distributed with some density ϱ with support on \mathbb{R}^+ . The family of distributions in Eq. (1b) has been extensively studied, for instance, by the physics community, in the context of *superstatistics* [3, 4]. It includes a large class of distributions with properties markedly different from the ones of Gaussians. For example, the inverse-Gamma distribution $\varrho(\Delta) = (2\pi\Delta^3)^{-1/2} e^{-\frac{1}{2\Delta}}$ leads to a d -dimensional Cauchy-like distribution $P(\mathbf{x}|\boldsymbol{\mu}) \propto (1 - \|\boldsymbol{\mu} - \mathbf{x}\|^2)^{-\frac{d+1}{2}}$, having as marginals Cauchy distributions and $\mathbb{E}[\|\mathbf{x} - \boldsymbol{\mu}\|^2] = +\infty$. We will perform our classification task by searching for a set of parameters (\mathbf{w}^*, b^*) , called respectively *weights* and *bias*, that will allow us to construct an estimator via a certain classifier $\varphi: \mathbb{R} \rightarrow \{-1, 1\}$

$$\mathbf{x} \mapsto \varphi\left(\frac{\mathbf{x}^\top \mathbf{w}^*}{\sqrt{d}} + b^*\right). \quad (2)$$

By means of the above law, we will predict the label for a new, unseen data point \mathbf{x} sampled from the same law $P(\mathbf{x}, y)$. Our analysis will be performed in the high-dimensional limit where both the sample size n and dimensionality d are sent to infinity, with $n/d \equiv \alpha$ kept constant.

Learning task In the most general setting, the parameters are estimated by minimising an empirical risk function in the form

$$(\mathbf{w}^*, b^*) \equiv \arg \min_{\substack{\mathbf{w} \in \mathbb{R}^d \\ b \in \mathbb{R}}} \mathcal{R}(\mathbf{w}, b) \quad \text{where} \quad \mathcal{R}(\mathbf{w}, b) \equiv \sum_{y=1}^n \ell\left(y^y, \frac{\mathbf{w}^\top \mathbf{x}^y}{\sqrt{d}} + b\right) + \lambda r(\mathbf{w}). \quad (3)$$

Here ℓ is a strictly convex loss function with respect to its second argument, and r is a strictly convex regularisation function with the parameter $\lambda \geq 0$ tuning its strength.

State evolution equations. Let us now present our main result, namely the exact asymptotic characterisation of the distribution of the estimator $\mathbf{w}^* \in \mathbb{R}^d$ and of $\frac{1}{\sqrt{d}}\mathbf{w}^{*\top}\mathbf{X} \in \mathbb{R}^n$, where $\mathbf{X} \in \mathbb{R}^{d \times n}$ is the concatenation of the n dataset column vectors $\mathbf{x}^\nu \in \mathbb{R}^d$, $\nu \in [n]$. Such an asymptotic characterisation is performed via a set of order parameters satisfying a system of self-consistent “state-evolution” equations, which we will solve numerically. The asymptotic expressions for generalisation and training errors, in particular, can be written in terms of such order parameters. In the following, we use the shorthand $\ell_\pm(u) \equiv \ell(\pm 1, u)$. Also, given a function $\Phi: \{-1, 1\} \rightarrow \mathbb{R}$, we will use the shorthand notation $\Phi_\pm \equiv \Phi(\pm 1)$ and denote $\mathbb{E}_\pm[\Phi_\pm] = \rho_+\Phi_+ + \rho_-\Phi_-$.

Let $\zeta \sim \mathcal{N}(0, 1)$ and $\Delta \sim \varrho$, both independent from other quantities. Let also be $\boldsymbol{\xi} \sim \mathcal{N}(\mathbf{0}, \mathbf{I}_d)$. Given $\phi_1: \mathbb{R}^d \rightarrow \mathbb{R}$ and $\phi_2: \mathbb{R}^n \rightarrow \mathbb{R}$, the estimator \mathbf{w}^* and the matrix $\mathbf{z}^* := \frac{1}{\sqrt{d}}\mathbf{w}^*\mathbf{X} \in \mathbb{R}^n$ verify:

$$\phi_1(\mathbf{w}^*) \xrightarrow[n, d \rightarrow +\infty]{\text{P}} \mathbb{E}_\xi [\phi_1(\mathbf{g})], \quad \phi_2(\mathbf{z}^*) \xrightarrow[n, d \rightarrow +\infty]{\text{P}} \mathbb{E}_\zeta [\phi_2(\mathbf{h})], \quad (4)$$

where we have introduced the proximal for the loss:

$$h_\pm = \arg \min_u \left[\frac{(u - \omega_\pm)^2}{2\Delta v} + \ell_\pm(u) \right], \quad \omega_\pm := m_\pm + b + \sqrt{q\Delta}\zeta \quad (5)$$

and $\mathbf{h} \in \mathbb{R}^n$ is obtained by concatenating ρ_+n quantities h_+ with ρ_-n quantities h_- . We have also introduced the proximal $\mathbf{g} \in \mathbb{R}^d$:

$$\mathbf{g} = \arg \min_{\mathbf{w}} \left(\hat{v} \frac{\|\mathbf{w}\|^2}{2} - \sqrt{d} \sum_{k=\pm} \hat{m}_k \mathbf{w}^\top \boldsymbol{\mu}_k - \sqrt{\hat{q}} \boldsymbol{\xi}^\top \mathbf{w} + \lambda r(\mathbf{w}) \right). \quad (6)$$

The collection of parameters $(b, q, m_\pm, v, \hat{q}, \hat{m}_\pm, \hat{v})$ appearing in the equations above is given by the fixed-point solution of the following self-consistent equations:

$$\begin{cases} m_\pm = \frac{1}{\sqrt{d}} \mathbb{E}_\xi [\mathbf{g}^\top \boldsymbol{\mu}_\pm], \\ q = \frac{1}{d} \mathbb{E}_\xi [\|\mathbf{g}\|^2], \\ v = \frac{1}{d} \hat{q}^{-1/2} \mathbb{E}_\xi [\mathbf{g}^\top \boldsymbol{\xi}], \end{cases} \quad \begin{cases} \hat{q} = \alpha \mathbb{E}_{\pm, \zeta, \Delta} [\Delta f_\pm^2], \\ \hat{v} = -\alpha q^{-1/2} \mathbb{E}_{\pm, \Delta, \zeta} [\sqrt{\Delta} f_\pm \zeta], \\ \hat{m}_\pm = \alpha \rho_\pm \mathbb{E}_{\Delta, \zeta} [f_\pm], \end{cases} \quad \begin{cases} f_\pm := \frac{h_\pm - \omega_\pm}{v\Delta}, \\ b = \mathbb{E}_{\pm, \Delta, \zeta} [h_\pm - m_\pm]. \end{cases} \quad (7)$$

As in the purely Gaussian case, the state evolution equations naturally split the dependence on the loss function ℓ , which is relevant in the computation of h_\pm , and on the regularisation function r , entering in the computation of \mathbf{g} . In the most general setting, we are required to solve two convex minimisation problems, consisting of the computation of the proximals h_\pm and \mathbf{g} [44]. As a consequence of the result above, the training loss ϵ_ℓ , the training error ϵ_t , and the test (or generalisation) error ϵ_g are given, in the proportional asymptotic limit, by

$$\begin{aligned} \frac{1}{n} \sum_{\nu=1}^n \ell\left(y^\nu, \frac{\mathbf{w}^{*\top} \mathbf{x}^\nu}{\sqrt{d}} + b^*\right) &\rightarrow \mathbb{E}_{\pm, \zeta, \Delta} [\ell_\pm(h_\pm)] =: \epsilon_\ell, \\ \frac{1}{n} \sum_{\nu=1}^n \mathbb{I}\left(\varphi\left(\frac{\mathbf{w}^{*\top} \mathbf{x}^\nu}{\sqrt{d}} + b^*\right) \neq y^\nu\right) &\rightarrow \mathbb{E}_{\pm, \zeta, \Delta} [\mathbb{I}(\varphi(h_\pm) \neq \pm 1)] =: \epsilon_t, \\ \mathbb{E}_{(y, \mathbf{x})} \left[\mathbb{I}\left(\varphi\left(\frac{\mathbf{w}^{*\top} \mathbf{x}}{\sqrt{d}} + b^*\right) \neq y\right) \right] &= \mathbb{E}_{\pm, \Delta, \zeta} [\mathbb{I}(\varphi(\omega_\pm) \neq \pm 1)] =: \epsilon_g. \end{aligned} \quad (8)$$

The derivation of the results above is given in Appendix A and is obtained via the replica method. Moreover, explicit forms for specific choices of ℓ or r highly simplify the equations in special cases. A very special case, in particular, is presented below.

Quadratic loss with ridge regularisation. As an example, let us consider the case of a quadratic loss, $\ell(y, x) = \frac{1}{2}(y - x)^2$ with ridge regularisation $r(\mathbf{w}) = \frac{1}{2}\|\mathbf{w}\|^2$. In this setting, an explicit formula for the proximal h_\pm in Eq. (5) and for the proximal \mathbf{g} in Eq. (6) can be easily found. As a result, we can obtain explicit expressions for the corresponding set of state evolution equations which become particularly suitable for a fast numerical solution:

$$\begin{cases} m_\pm = \frac{\sum_{k=\pm} \hat{m}_k \boldsymbol{\mu}_k^\top \boldsymbol{\mu}_\pm}{\lambda + \hat{v}}, \\ q = \frac{\|\sum_{k=\pm} \hat{m}_k \boldsymbol{\mu}_k\|^2 + \hat{q}}{(\lambda + \hat{v})^2}, \\ v = \frac{1}{\lambda + \hat{v}}, \end{cases} \quad \begin{cases} \hat{q} = \alpha \mathbb{E}_\pm [(\pm 1 - m_\pm - b)^2] \mathbb{E}_\Delta \left[\frac{\Delta}{(1 + v\Delta)^2} \right] + \alpha q \mathbb{E}_\Delta \left[\frac{\Delta^2}{(1 + v\Delta)^2} \right], \\ \hat{v} = \alpha \mathbb{E}_\Delta \left[\frac{\Delta}{1 + v\Delta} \right], \\ \hat{m}_\pm = \alpha \rho_\pm (\pm 1 - m_\pm - b) \mathbb{E}_\Delta \left[\frac{1}{1 + v\Delta} \right]. \end{cases} \quad (9)$$

3 Application to synthetic datasets

In this section, we compare our theoretical predictions with the results of numerical experiments for a large family of data distributions. The results have been obtained using ridge ℓ_2 -regularisation, and both quadratic and logistic losses, with various data cluster balances ρ . We will also assume, without loss of generality, that $\boldsymbol{\mu}_\pm = \pm \frac{1}{\sqrt{d}}\boldsymbol{\mu}$, where $\boldsymbol{\mu}$ is extracted from a distribution $\mathcal{N}(\mathbf{0}, \mathbf{I}_d)$. Our artificial data sets will be produced using, for the Δ distribution ϱ , an inverse-Gamma distribution parametrised as

$$\varrho(\Delta) \equiv \varrho_{a,c}(\Delta) = \frac{c^a}{\Gamma(a)\Delta^{a+1}} e^{-\frac{c}{\Delta}}, \quad (10a)$$

depending on the shape parameter $a > 0$ and on the scale parameter $c > 0$. As a result, each class will be distributed as

$$P(\mathbf{x}|\boldsymbol{\mu}) = \frac{(2c)^a \Gamma(a + \frac{d}{2})}{\Gamma(a) \pi^{\frac{d}{2}}} (2c + \|\mathbf{x} - \boldsymbol{\mu}\|^2)^{-a - \frac{d}{2}}, \quad (10b)$$

which produces a cloud centered in $\boldsymbol{\mu}$. The reason for our choice is that the distribution $\varrho_{a,c}$ allows us to easily explore different regimes by changing two parameters only. Indeed, the distribution has, for $a > 1$, covariance matrix $\boldsymbol{\Sigma} = \mathbb{E}[(\mathbf{x} - \boldsymbol{\mu}) \otimes (\mathbf{x} - \boldsymbol{\mu})^\top] = \sigma^2 \mathbf{I}_d$, where $\sigma^2 = \frac{c}{a-1}$. By fixing σ^2 and taking the limit $a \rightarrow +\infty$, $P(\mathbf{x}|\boldsymbol{\mu}) \rightarrow \mathcal{N}(\mathbf{x}|\boldsymbol{\mu}, \sigma^2 \mathbf{I}_d)$, i.e., the Gaussian case discussed by Mignacco et al. [37]. For $a \in (0, 1]$, instead, $\sigma^2 = +\infty$. Note that the choice of inverse-Gamma distribution for ϱ is not that unusual. It has been adopted, for example, to describe non-Gaussian data in quantitative finance [11, 28] or econometrics models [40]. Finally, we will construct our label estimator as in Eq. (2) with $\varphi(x) = \text{sign}(x)$.

3.1 Finite-covariance case

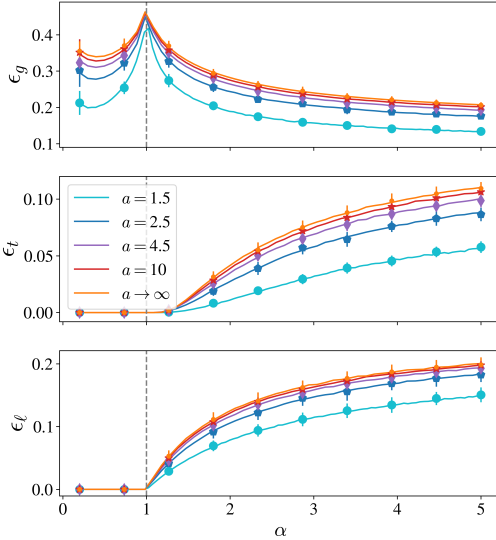


Figure 1: Test error ϵ_g (top), training error ϵ_t (center) and training loss ϵ_ℓ (bottom) as predicted by Eq. (8) in the balanced $\rho = 1/2$ case. The dataset distribution is parametrised as in Eq. (11). The classification task is solved using a quadratic loss with ridge regularisation with $\lambda = 10^{-5}$. Dots correspond to the average outcome of 50 numerical experiments in dimension $d = 10^3$. In our parametrisation, the population covariance is $\boldsymbol{\Sigma} = \mathbf{I}_d$ for all values of a and moreover, for $a \rightarrow +\infty$, the case of Gaussian clouds with the same centroids and covariance is recovered. For further details on the numerical solutions, see Appendix B.

The plot shows that, at given population covariance

Let us start by considering a data set distribution as in Eq. (10) with shape parameter $a = c+1 > 1$. The data set distribution in this case is given by

$$P(\mathbf{x}|\boldsymbol{\mu}) = \frac{2^a (a-1)^a \Gamma(a + \frac{d}{2})}{\Gamma(a) \pi^{\frac{d}{2}}} (2a - 2 + \|\mathbf{x} - \boldsymbol{\mu}\|^2)^{-a - \frac{d}{2}} \quad (11)$$

and decays as $\|\mathbf{x}\|^{-2a-1}$ in the radial direction for $\|\mathbf{x} - \boldsymbol{\mu}\| \gg 0$. As a consequence, the distribution has $\lim_{d \rightarrow \infty} \frac{1}{d} \mathbb{E}[\|\mathbf{x} - \boldsymbol{\mu}\|^k] = +\infty$ for $k \geq 2a$. With this choice, all elements of the family in Eq. (11) have the same covariance $\boldsymbol{\Sigma} = \mathbb{E}[(\mathbf{x} - \boldsymbol{\mu}) \otimes (\mathbf{x} - \boldsymbol{\mu})^\top] = \mathbf{I}_d$ as a is varied, including the Gaussian limit $P(\mathbf{x}|\boldsymbol{\mu}) \rightarrow \mathcal{N}(\boldsymbol{\mu}, \mathbf{I}_d)$ obtained for $a \rightarrow +\infty$.

In Fig. 1 we present the results of our numerical experiments using the square loss and small regularisation. An excellent agreement between the theoretical predictions and the results of numerical experiments is found for a range of values of a and sample complexity α , both for balanced, i.e., equally sized, and unbalanced clusters of data (the plot for this case can be found in Appendix A.3). The test error ϵ_g presents the classical interpolation peak at $\alpha = 1$, slightly smoothed by the presence of a non-zero regularisation strength λ , and the typical double-descent behavior [41]. As a is increased, the results of Mignacco et al. [37] for Gaussian clouds with $P(\mathbf{x}|\boldsymbol{\mu}) = \mathcal{N}(\mathbf{x}|\boldsymbol{\mu}, \mathbf{I}_d)$ are recovered. The $a \rightarrow +\infty$ curves correspond, therefore, to the Gaussian mixture model we would have constructed by simply fitting the first and second

$\Sigma = \mathbf{I}_d$, the classification of power-law distributed clouds has a different, and in particular smaller, test error than the corresponding task on Gaussian clouds with the same covariance: in this sense, no Gaussian universality principle holds. This (perhaps) counter-intuitive effect stems from the fact that, although for all classes $\Sigma = \mathbf{I}_d$, the mean absolute deviation is smaller for finite a

$$\lim_{d \rightarrow +\infty} \frac{\mathbb{E}[\|x - \mu\|]}{\sqrt{\mathbb{E}[\|x - \mu\|^2]}} = \frac{\Gamma(a-1/2)\sqrt{a-1}}{\Gamma(a)} \xrightarrow{a \rightarrow +\infty} 1^- . \quad (12)$$

The learning process benefits from the fact that points are on average closer to their means μ_{\pm} , although the fat tails produce the same variance. Finally, we observed that test errors are systematically smaller for unbalanced clusters than for balanced clusters (see Appendix A.3).

The same numerical experiment has been repeated using the logistic loss for training. Once again, in Fig. 2, we focus on $\rho = 1/2$ and show that the theoretical predictions of the generalisation and training errors agree with the results of numerical experiments for a range of sample complexity values α and various values of a . Just as for the square loss, the test error ϵ_g of the Gaussian model ($a \rightarrow +\infty$) is larger than the one observed for power-law distributed clouds at finite values of a . In the $\lambda \rightarrow 0$ limit, the typical interpolation cusp in the generalisation error is observed: the cusp occurs at different values of α as a is changed; interpolation occurs at smaller values of α for larger a (i.e., for “more Gaussian” distributions). A comparison with the test error ϵ_t confirms that this cusp occurs at the value of α where the training error becomes non-zero and the two training data clouds become non-separable [53, 12]. This sharp transition in α also corresponds to the existence transition of maximum-likelihood estimator in high-dimensional logistic regression for Gaussian data as shown by Sur and Candès [53]. For larger regularisation strength, the cusp smoothens, and the training error becomes non-zero at smaller values of α .

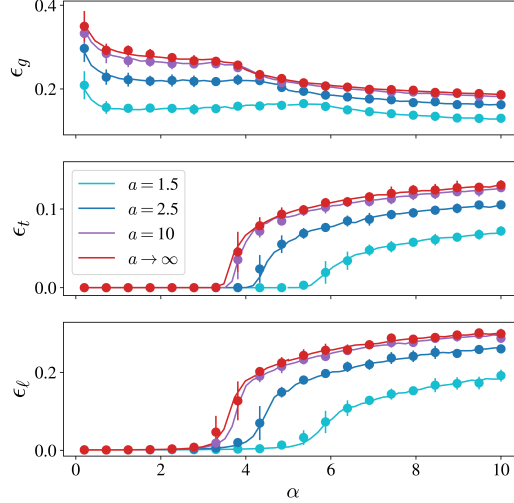


Figure 2: Test error ϵ_g (top), training error ϵ_t (center) and training loss ϵ_l (bottom) via logistic loss training on balanced clusters parametrised as in Eq. (11) ($\Sigma = \mathbf{I}_d$). A ridge regularisation with $\lambda = 10^{-4}$ is adopted. Dots correspond to the average over 20 numerical experiments with $d = 10^3$. The Gaussian limit is recovered for $a \rightarrow +\infty$. Further details on the numerical solutions can be found in Appendix B.

3.2 Infinite-covariance case

The family of distributions specified by Eq. (10) allows us to also consider the case of infinite covariance, i.e., $\sigma^2 = +\infty$. To test our formulas in this setting, we considered a superposition of a Gaussian mixture and a mixture of infinite-covariance distributions obtained using Eq. (10b) with $c = 1$ and $a = 1/2$ for the square loss, and $a = 3/4$ for the logistic loss. In other words, we adopted as dataset distribution the density $\varrho(\Delta) = r\varrho_{a,1}(\Delta) + (1-r)\delta(\Delta-1)$, with $r \in [0, 1]$ interpolation parameter, for Δ in Eq. (1). The mixture has infinite covariance for $0 < r \leq 1$ and the Gaussian limit is recovered for $r = 0$. Fig. 3 collects our results for two balanced clouds. Good agreement between the theoretical predictions and the results of numerical experiments is found for a range of values of sample complexity and of the ratio r . In this case, the finite-variance case $r = 0$ corresponds, not surprisingly, to the lowest test error with both square loss and logistic loss.

3.3 The role of regularisation in the classification of non-Gaussian clouds

One of the main results in the work of Mignacco et al. [37] is related to the effect of regularisation on the performances in a classification task on a Gaussian mixture. They observed that, for all values of the sample complexity α , the optimal ridge classification performance on a pair of balanced clouds is obtained for an infinite regularisation strength λ , using both hinge loss and square loss. We tested the robustness of this result beyond the purely Gaussian setting. In Fig. 4 (left), we plot the test error obtained using square loss and different regularisation strengths λ on the dataset distribution as in

Eq. (11) with $a = 2$. We observe that, both in the balanced case and in the unbalanced case, the optimal regularisation strength λ^* is *finite* and, moreover, α -dependent. On the other hand, if we fix α and let a grow towards $+\infty$, the optimal λ^* grows as well to recover the result of Mignacco et al. [37] of diverging optimal regularisation for balanced Gaussian clouds, as shown in Fig. 4 (center). Therein, we fix $\alpha = 2$ and we extract, for each value of a , the value of λ^* that minimises the test error ϵ_g in the case of balanced clusters, showing that it is indeed finite for finite a and diverges as $a \rightarrow +\infty$, see Fig. 4 (right). Fig. 4 (right) also shows that, in the unbalanced case, the optimal regularisation strength λ^* saturates for $a \rightarrow +\infty$ to a finite value, as for Gaussian clouds [37].

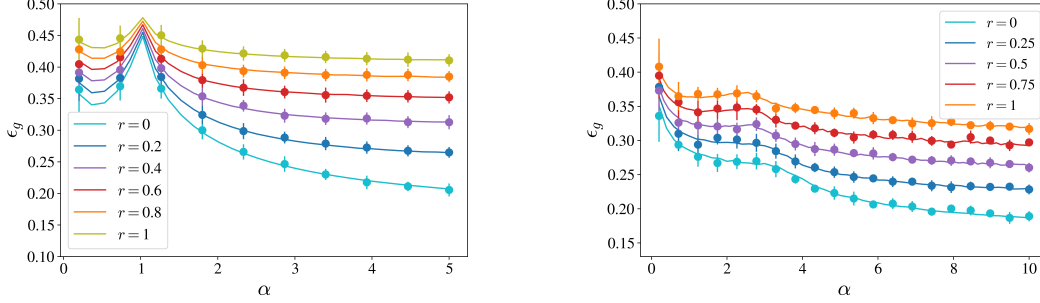


Figure 3: Test error ϵ_g in the classification of two balanced clouds via quadratic loss (*left*) and logistic loss (*right*). In both cases, ridge regularisation is adopted ($\lambda = 10^{-4}$ for the square loss case, $\lambda = 10^{-3}$ for the logistic loss case). Each cloud is a superposition of a power-law distribution with infinite variance and a Gaussian with covariance $\Sigma = \mathbf{I}_d$. The parameter r allows us to interpolate between the purely Gaussian limit ($r = 0$) and the infinite-variance limit ($0 < r \leq 1$). Dots correspond to the average test error of 20 numerical experiments in dimension $d = 10^3$. Note that, at a given sample complexity, Gaussian clouds are associated with the lowest test error for both losses.

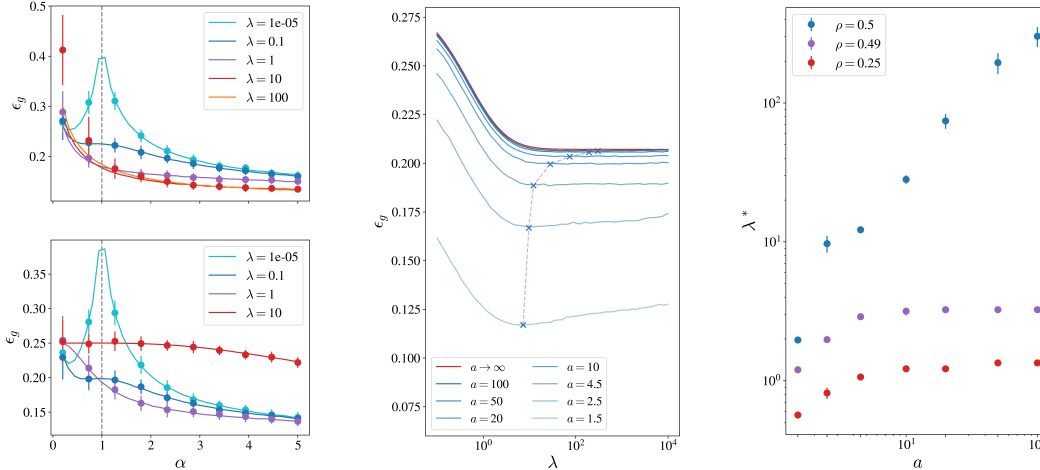


Figure 4: (*Left*) Test error for ridge regularised quadratic loss for various regularisation strengths. The data points of each cloud in the training set are distributed as in Eq. (11), with shape parameter $a = 2$, for balanced clusters (*top*) and unbalanced clusters ($\rho = 1/4$, *bottom*). Points are the results of 50 numerical experiments. (*Center*) Test error for different regularisation strengths λ for two *balanced* clusters with quadratic loss at sample complexity $\alpha = 2$ using the data distribution (11). The optimal regularisation strength value λ^* obtained from averaging 5 runs for each a is marked with a cross. (*Right*) Optimal regularisation strength λ^* at $\alpha = 2$ for different values of $a \in [1.5, 10^2]$ for both balanced and unbalanced clusters, obtained from averaging 5 runs. Note that, for $\rho = 1/2$, $\lambda^* \rightarrow +\infty$ as $a \rightarrow +\infty$.

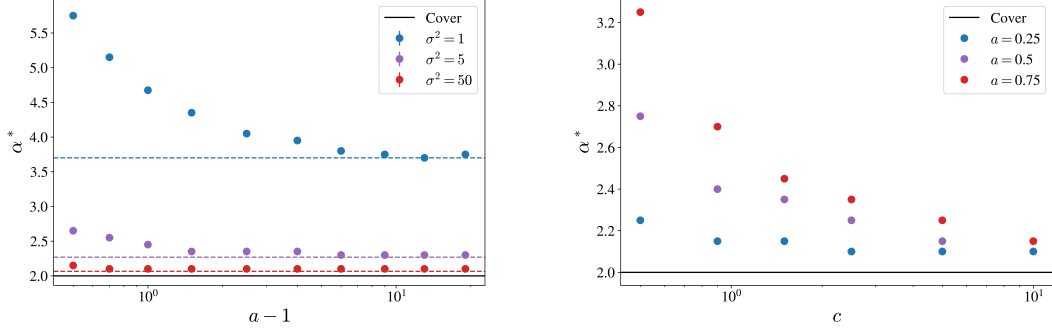


Figure 5: Separability threshold α^* obtained by solving the equations in Eq. (7) with logistic loss, ridge regularisation strength $\lambda = 10^{-5}$ and $\rho = 1/2$. The data points of each cloud are distributed around their mean $\boldsymbol{\mu}$ with a two-parameter distribution as in Eq. (10b). (Left) Finite covariance $\boldsymbol{\Sigma} = \sigma^2 \mathbf{I}_d$ case, $\sigma^2 = \frac{c}{a-1}$, as a function of a . Dashed lines are the threshold values of the Gaussian case [37]. At large a and large variance σ^2 , the Cover’s transition $\alpha = 2$ for balanced clusters (black line) is recovered. (Right) Infinite-variance data clusters case. The cluster distribution is obtained by fixing $0 < a < 1$ in Eq. (10b).

3.4 The separability threshold

By studying the training error ϵ_t with logistic loss at zero regularisation we can obtain information on the boundary between the region in which the training data are perfectly separable and the regime in which they are not. In other words, we can extract the value of the so-called separability transition complexity α^* [53, 37, 31]. Once again, a complete characterisation of this transition point is available in the Gaussian mixture case, where α^* can be explicitly given as a function of σ^2 [37].

It is not trivial to extend such a result to the general case of non-Gaussian mixtures (including the case of a mixture of distributions with infinite covariance). It is however possible to estimate α^* within the large family of “superstatistical” models we are considering here by a direct computation of ϵ_t . Fig. 5 shows the values of α^* for different choices of the shape parameters a and c in the case of two balanced clouds of datapoints distributed as in Eq. (10b). The value is obtained by solving the state evolution equations in Eq. (7) with negligible ridge regularisation strength, and by recording the largest value of sample complexity associated with zero training error. In Fig. 5 (left), we fixed $\sigma^2 = \frac{c}{a-1} < +\infty$, and plotted the separability threshold α^* for a range of values of the shape parameter $a > 1$. As a grows, the Gaussian mixture case is recovered, and therefore the corresponding known α^* [37]. The double limit $a \rightarrow \infty$ and $\sigma^2 \rightarrow \infty$, on the other hand, provides the Cover [8] transition value $\alpha^* = 2$, as expected. In Fig. 5 (right), instead, we analyse the case of infinite-variance clusters, by fixing $a \in (0, 1)$ and by varying the scale parameter c in Eq. (10b). In this setting, c plays the role of distribution width. The Cover transition is therefore correctly recovered as c diverges for all values of a . Finding an explicit formula for α^* in this setting remains an open problem for future works.

3.5 Random labels and Gaussian universality

Our analysis can be extended to the case in which a point \mathbf{x} is labeled by a “teacher”, represented by a probabilistic law $P_0(y|\tau)$ and a vector $\boldsymbol{\theta}_0 \in \mathbb{R}^d$ so that each dataset element is independently generated with the joint distribution

$$P(\mathbf{x}, y) = P_0\left(y \left| \frac{\boldsymbol{\theta}_0^\top \mathbf{x}}{\sqrt{d}}\right.\right) \sum_{k=\pm} \rho_k \mathbb{E}[\mathcal{N}(\mathbf{x} | \boldsymbol{\mu}_k, \Delta \mathbf{I}_d)]. \quad (13)$$

Let us assume now that $P_0(y|\tau) = P_0(-y | -\tau)$ and that $\boldsymbol{\theta}_0$ is such that $\lim_{d \rightarrow \infty} \frac{1}{\sqrt{d}} \boldsymbol{\theta}_0^\top \boldsymbol{\mu}_\pm = 0$. In Appendix A.4 we show that, if $\ell(y, \eta) = \ell(-y, -\eta)$, the task is equivalent to a classification problem on a *single* cloud centered in the origin, i.e., to the case $\boldsymbol{\mu}_\pm = \mathbf{0}$, so that $P(\mathbf{x}, y) = P_0(y | \frac{1}{\sqrt{d}} \boldsymbol{\theta}_0^\top \mathbf{x}) \mathbb{E}[\mathcal{N}(\mathbf{x} | \mathbf{0}, \Delta \mathbf{I}_d)]$. This mean-invariance has been recently proven in Ref. [17] in the pure Gaussian setting and extends therefore to a non-Gaussian mixture. The condition $\lim_{d \rightarrow \infty} \frac{1}{\sqrt{d}} \boldsymbol{\theta}_0^\top \boldsymbol{\mu}_\pm = 0$ essentially expresses the independence of the teacher’s labeling criterion from the dataset structure.

A special, relevant case of “uncorrelated teacher” is the one of *random labels*, where $P_0(y|\tau) = 1/2(\delta_{y,+1} + \delta_{y,-1})$. This apparently vacuous model is relevant in the study of the storage capacity problem [16, 27, 7] and of the separability threshold [8], and it has also been an effective tool to better understand deep learning [33, 56]. By tackling this setting using the square loss $\ell(y, \eta) = 1/2(y - \eta)^2$, we show in Appendix A.4 that, in the limit of zero ridge regularisation $\lambda \rightarrow 0^+$, the training loss is *independent of the distribution of Δ* , and given by the universal formula

$$\frac{1}{2n} \sum_{y=1}^{\infty} \left(y^y - \frac{\mathbf{x}^\top \mathbf{w}^\star}{\sqrt{d}} \right)^2 \xrightarrow[n/a=\alpha]{n \rightarrow +\infty} \frac{\alpha-1}{2\alpha} \theta(\alpha-1) =: \epsilon_\ell. \quad (14)$$

Note that this result does not require $\sigma^2 := \mathbb{E}[\Delta]$ to be finite, and it includes, as a special case, the Gaussian mixture model with random labels considered in Ref. [17, 46]. Therein, Eq. (14) has been obtained under the Gaussian design hypothesis. It turns out therefore that Eq. (14) holds for a much larger ensemble, which includes fat-tailed distributions with possibly infinite covariance. On the other hand, universality *does not* hold, e.g., for the training error.

In Fig. 6 we exemplify these results by using ridge-regularised square loss. The numerical experiments correspond to a classification task on a dataset of *two* clouds centered in $\boldsymbol{\mu}_\pm$, $\boldsymbol{\mu}_+ = -\boldsymbol{\mu}_- \sim \mathcal{N}(\mathbf{0}, 1/a \mathbf{I}_d)$, obtained using the distribution

$$P(\mathbf{x}, y) = \frac{\delta_{y,+1} + \delta_{y,-1}}{4} \sum_{k=\pm} P(\mathbf{x}|\boldsymbol{\mu}_k), \quad (15)$$

where $P(\mathbf{x}|\boldsymbol{\mu}_\pm)$ is the distribution in Eq. (10b) depending on the shape parameters a and c . These results are compared with the theoretical prediction obtained for a *single* cloud, with the same parameters a and c , but centered in the origin, so that $P(\mathbf{x}, y) = \frac{\delta_{y,+1} + \delta_{y,-1}}{2} P(\mathbf{x}|\mathbf{0})$: the agreement confirms the “mean-invariance” property stated above. As anticipated, as we are considering random labels, the training loss ϵ_ℓ follows Eq. (14) in all cases, whereas the test error is not universal. Note that, in place of the test error (which is trivially $\epsilon_g = 1/2$) we plot the mean square error $\hat{\epsilon}_g := \mathbb{E}_{(y, \mathbf{x})} [(y - 1/\sqrt{a} \mathbf{x}^\top \mathbf{w}^\star)^2]$. Also, observe that this quantity is divergent in the case of infinite covariance, hence is absent from the plot for $a \in (0, 1]$.

Acknowledgements

The authors would like to thank Nikolas Nüsken for stimulating discussions. Also, we would like to thank Bruno Loureiro for his feedback and for his careful reading of the manuscript.

References

- [1] R.J. Adler, R.E. Feldman, and M.S. Taqqu, editors. *A Practical Guide to Heavy Tails: Statistical Techniques and Applications*. Birkhauser Boston Inc., USA, 1998. ISBN 0817639519.
- [2] C. Baldassi, E.M. Malatesta, M. Negri, and R. Zecchina. Wide flat minima and optimal generalization in classifying high-dimensional gaussian mixtures. *J. Stat. Mech.: Theory Exp.*, 2020(12):124012, 2020.

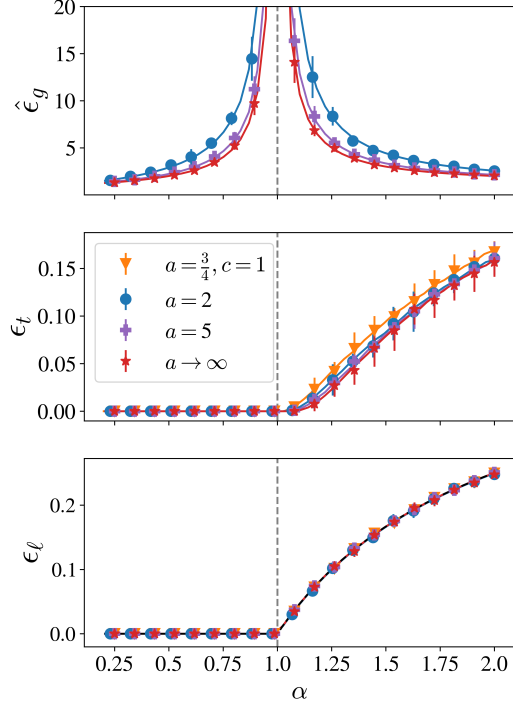


Figure 6: Mean square error $\hat{\epsilon}_g$ (top), training error ϵ_t (center) and training loss ϵ_ℓ (bottom) obtained using square loss on a dataset distributed as in Eq (15) with random labels (dots) compared with the theoretical predictions for the single cluster case (continuous lines). The distributions are parametrised using Eq. (11) for $a > 1$ and Eq. (10b) for $0 < a \leq 1$. A ridge regularisation with $\lambda = 10^{-4}$ is adopted. Note that $\hat{\epsilon}_g$ is absent in the top plot for $a = 1/2$ and $c = 1$ being a divergent quantity in this case.

- [3] C. Beck. Superstatistics: Theory and applications. *Contin. Mech. Thermodyn.*, 16, 03 2003.
- [4] C. Beck and E.G.D. Cohen. Superstatistics. *Physica A*, 322:267–275, 2003.
- [5] M. Belkin, D. Hsu, S. Ma, and S. Mandal. Reconciling modern machine-learning practice and the classical bias–variance trade-off. *Proc. Natl. Acad. Sci. U.S.A.*, 116(32):15849–15854, 2019.
- [6] M. Belkin, A. Rakhlin, and A.B. Tsybakov. Does data interpolation contradict statistical optimality? In K. Chaudhuri and M. Sugiyama, editors, *Proceedings of the 22nd International Conference on Artificial Intelligence and Statistics*, volume 89 of *Proc. Mach. Learn. Res.*, pages 1611–1619. PMLR, 2019.
- [7] N. Brunel, J.-P. Nadal, and G. Toulouse. Information capacity of a perceptron. *JJ. Phys. A: Math. Gen.*, 25(19):5017, oct 1992.
- [8] T.M. Cover. Geometrical and statistical properties of systems of linear inequalities with applications in pattern recognition. *IEEE Trans. Comput.*, EC-14(3):326–334, 1965.
- [9] Yatin Dandi, Ludovic Stephan, Florent Krzakala, Bruno Loureiro, and Lenka Zdeborová. Universality laws for gaussian mixtures in generalized linear models. *arXiv:2302.08933*, 2023.
- [10] P. del Giudice, S. Franz, and M. Virasoro. Perceptron beyond the limit of capacity. *J. Physique*, 50:121–134, 01 1989.
- [11] D. Delpini and G. Bormetti. Minimal model of financial stylized facts. *Phys. Rev. E*, 83:041111, 2011.
- [12] A. Deng, Z. Kammoun and C. Thrampoulidis. A model of double descent for high-dimensional binary linear classification. *Inf. Inference*, 11, 2021.
- [13] N. El Karoui. On the impact of predictor geometry on the performance on high-dimensional ridge-regularized generalized robust regression estimators. *Probab. Theory Relat. Fields*, 170, 2018.
- [14] S. Franz, D.J. Amit, and M.A. Virasoro. Prosopagnosia in high capacity neural networks storing uncorrelated classes. *J. Physique*, 51(5):387–408, 1990.
- [15] E Gardner. The space of interactions in neural network models. *J. Phys. A: Math. Gen.*, 21(1): 257, 1988.
- [16] E. Gardner and B. Derrida. Three unfinished works on the optimal storage capacity of networks. *J. Phys. A: Math. Gen.*, 22(12):1983, 1989.
- [17] F. Gerace, F. Krzakala, B., L. Stephan, and L. Zdeborová. Gaussian universality of perceptrons with random labels. *arXiv:2205.13303*.
- [18] F. Gerace, B. Loureiro, F. Krzakala, M. Mézard, and L. Zdeborová. Generalisation error in learning with random features and the hidden manifold model. In *ICML*, pages 3452–3462, 2020.
- [19] B. Ghorbani, S. Mei, T. Misiakiewicz, and A. Montanari. Limitations of lazy training of two-layers neural network. In H. Wallach, H. Larochelle, A. Beygelzimer, F. d'Alché-Buc, E. Fox, and R. Garnett, editors, *Advances in Neural Information Processing Systems*, volume 32, 2019.
- [20] S. Goldt, M. Mézard, F. Krzakala, and L. Zdeborová. Modeling the influence of data structure on learning in neural networks: The hidden manifold model. *Phys. Rev. X*, 10:041044, Dec 2020.
- [21] S. Goldt, M. Mézard, F. Krzakala, and L. Zdeborová. Modeling the influence of data structure on learning in neural networks: The hidden manifold model. *Phys. Rev. X*, 10:041044, 2020.
- [22] T. Hastie, R. Tibshirani, and J.H. Friedman. *The elements of statistical learning: data mining, inference, and prediction*, volume 2. Springer, 2009.

- [23] T. Hastie, A. Montanari, S. Rosset, and R.J. Tibshirani. Surprises in high-dimensional ridgeless least squares interpolation. *Ann. Stat.*, 50(2):949 – 986, 2022.
- [24] H. Hu and Y.M. Lu. Universality laws for high-dimensional learning with random features. *arXiv:2009.07669*, 2022.
- [25] G.R. Kini and C. Thrampoulidis. Phase transitions for one-vs-one and one-vs-all linear separability in multiclass gaussian mixtures. In *ICASSP 2021*, pages 4020–4024, 2021.
- [26] V. Kothapalli, E. Rasromani, and V. Awatramani. Neural collapse: A review on modelling principles and generalization. *arXiv:2206.04041*, 2022.
- [27] W. Krauth and M. Mézard. Storage capacity of memory networks with binary couplings. *J. Physique*, 50(20):3057–3066, 1989.
- [28] N. Langrené, G. Lee, and Z. Zhu. Switching to non-affine stochastic volatility: A closed-form expansion for the inverse gamma model. *Int. J. Theor. Appl. Finance*, 19, 2015.
- [29] M. Lelarge and L. Miolane. Asymptotic bayes risk for gaussian mixture in a semi-supervised setting. In *2019 IEEE 8th International Workshop on Computational Advances in Multi-Sensor Adaptive Processing*, pages 639–643, 2019.
- [30] M. Lelarge and L. Miolane. Asymptotic bayes risk for gaussian mixture in a semi-supervised setting. In *2019 IEEE 8th International Workshop on Computational Advances in Multi-Sensor Adaptive Processing (CAMSAP)*, pages 639–643, 2019.
- [31] B. Loureiro, G. Sicuro, C. Gerbelot, A. Pacco, F. Krzakala, and L. Zdeborová. Learning Gaussian Mixtures with Generalized Linear Models: Precise Asymptotics in High-dimensions. *Advances in Neural Information Processing Systems*, 34:10144–10157, 2021.
- [32] B. Loureiro, C. Gerbelot, H. Cui, S. Goldt, F. Krzakala, M. Mézard, and L. Zdeborová. Learning curves of generic features maps for realistic datasets with a teacher-student model. *J. Stat. Mech.: Theory Exp.*, 2022(11):114001, 2022.
- [33] H. Maennel, I.M. Alabdulmohsin, I.O. Tolstikhin, R. Baldock, O. Bousquet, S. Gelly, and D. Keysers. What do neural networks learn when trained with random labels? In H. Larochelle, M. Ranzato, R. Hadsell, M.F. Balcan, and H. Lin, editors, *Advances in Neural Information Processing Systems*, volume 33, pages 19693–19704. Curran Associates, Inc., 2020.
- [34] X. Mai and Z. Liao. High dimensional classification via regularized and unregularized empirical risk minimization: Precise error and optimal loss. *arXiv:1905.13742*, 2020.
- [35] S. Mei and A. Montanari. The Generalization Error of Random Features Regression: Precise Asymptotics and the Double Descent Curve. *Commun. Pure Appl. Math.*, 75, 2019.
- [36] M. Mézard, G. Parisi, and M.A. Virasoro. *Spin glass theory and beyond: An Introduction to the Replica Method and Its Applications*, volume 9. World Scientific Publishing Company, 1987.
- [37] F. Mignacco, F. Krzakala, Y. Lu, P. Urbani, and L. Zdeborová. The role of regularization in classification of high-dimensional noisy Gaussian mixture. In Hal Daumé III and Aarti Singh, editors, *Proceedings of the 37th International Conference on Machine Learning*, volume 119 of *Proc. Mach. Learn. Res.*, pages 6874–6883. PMLR, 13–18 Jul 2020.
- [38] A. Montanari and P.-M. Nguyen. Universality of the elastic net error. In *2017 IEEE ISIT*, pages 2338–2342. IEEE, 2017.
- [39] A. Montanari and B.N. Saeed. Universality of empirical risk minimization. In Po-Ling Loh and Maxim Raginsky, editors, *Proceedings of 35th Conference on Learning Theory*, volume 178 of *Proceedings of Machine Learning Research*, pages 4310–4312. PMLR, 02–05 Jul 2022.
- [40] D.B. Nelson. Arch models as diffusion approximations. *J. Econom.*, 45(1-2):7–38, 1990.
- [41] M. Opper, W. Kinzel, J. Kleinz, and R. Nehl. On the ability of the optimal perceptron to generalise. *J. Phys. A: Math. Gen.*, 23(11):L581, jun 1990.

- [42] A. Panahi and B. Hassibi. A universal analysis of large-scale regularized least squares solutions. In I. Guyon, U. Von Luxburg, S. Bengio, H. Wallach, R. Fergus, S. Vishwanathan, and R. Garnett, editors, *Advances in Neural Information Processing Systems*, volume 30. Curran Associates, Inc., 2017.
- [43] V. Pappayan, X.Y. Han, and D.L. Donoho. Prevalence of neural collapse during the terminal phase of deep learning training. *Proc. Natl. Acad. Sci. U.S.A.*, 117(40):24652–24663, 2020.
- [44] N. Parikh and S. Boyd. Proximal algorithms. *Found. Trends Optim.*, 1(3):127–239, jan 2014.
- [45] F. Pedregosa, G. Varoquaux, A. Gramfort, V. Michel, B. Thirion, O. Grisel, M. Blondel, P. Prettenhofer, R. Weiss, V. Dubourg, J. Vanderplas, A. Passos, D. Cournapeau, M. Brucher, M. Perrot, and E. Duchesnay. Scikit-learn: Machine learning in Python. *J. Mach. Learn. Res.*, 12:2825–2830, 2011.
- [46] L. Pesce, F. Krzakala, B. Loureiro, and L. Stephan. Are Gaussian data all you need? Extents and limits of universality in high-dimensional generalized linear estimation. *arXiv:2302.08923*, 2023.
- [47] A. Rahimi and B. Recht. Random features for large-scale kernel machines. In J. Platt, D. Koller, Y. Singer, and S. Roweis, editors, *Advances in Neural Information Processing Systems*, volume 20. Curran Associates, Inc., 2007.
- [48] W.J. Reed and B.D. Hughes. From gene families and genera to incomes and internet file sizes: Why power laws are so common in nature. *Phys. Rev. E*, 66:067103, Dec 2002.
- [49] S. Rosset, J. Zhu, and T. Hastie. Margin maximizing loss functions. In S. Thrun, L. Saul, and B. Schölkopf, editors, *Advances in Neural Information Processing Systems*, volume 16. MIT Press, 2003.
- [50] M.E.A. Seddik, C. Louart, M. Tamaazousti, and R. Couillet. Random matrix theory proves that deep learning representations of GAN-data behave as Gaussian mixtures. In H.D. III and A. Singh, editors, *Proceedings of the 37th International Conference on Machine Learning*, volume 119 of *Proc. Mach. Learn. Res.*, pages 8573–8582. PMLR, 13–18 Jul 2020.
- [51] H. S. Seung, H. Sompolinsky, and N. Tishby. Statistical mechanics of learning from examples. *Phys. Rev. A*, 45:6056–6091, 1992.
- [52] L. Steinberger and H. Leeb. Conditional predictive inference for stable algorithms.
- [53] P. Sur and E.J. Candès. A modern maximum-likelihood theory for high-dimensional logistic regression. *Proc. Natl. Acad. Sci. U.S.A.*, 116(29):14516–14525, 2019.
- [54] C. Thrampoulidis, E. Abbasi, and B. Hassibi. Precise error analysis of regularized m -estimators in high dimensions. *IEEE Trans. Inf. Theory*, 64(8):5592–5628, 2018.
- [55] T.L.H. Watkin, A. Rau, and M. Biehl. The statistical mechanics of learning a rule. *Rev. Mod. Phys.*, 65:499–556, 1993.
- [56] C. Zhang, S. Bengio, M. Hardt, B. Recht, and O. Vinyals. Understanding deep learning (still) requires rethinking generalization. *Commun. ACM*, 64(3):107–115, feb 2021.
- [57] Q. Zhao, P. Sur, and E.J. Candès. The asymptotic distribution of the MLE in high-dimensional logistic models: Arbitrary covariance. *Bernoulli*, 28(3):1835 – 1861, 2022.

A Derivation of the fixed-point equations

In this Appendix, we will derive the fixed-point equations for the order parameters presented in the main text, following and generalising the analysis in Ref. [31]. The dataset $\mathcal{D} := \{(\mathbf{x}^v, y^v)\}_{v \in [n]}$ we are going to consider consists of n independent datapoints $\mathbf{x}^v \in \mathbb{R}^d$ each associated with a label $y^v \in \{-1, 1\} = \mathcal{Y}$. The elements of the dataset are independently generated by using a law $P(\mathbf{x}, y)$ which we assume can be put in the form $P(\mathbf{x}, y) \equiv \int_0^\infty P(\mathbf{x}, y|\Delta) \varrho(\Delta) d\Delta$ for some given distribution on the positive real axis ϱ , and such that

$$P(\mathbf{x}, \pm 1|\Delta) = \rho_\pm \mathcal{N}(\mathbf{x} | \boldsymbol{\mu}_\pm, \Delta \mathbf{I}_d), \quad \rho_+, \rho_- \in (0, 1), \quad \rho_+ + \rho_- = 1. \quad (16)$$

The vectors $\boldsymbol{\mu}_\pm \in \mathbb{R}^d$ play the role of centroids of two clusters labeled by $y = +1$ and $y = -1$, respectively. We will perform our classification task searching for a set of parameters (\mathbf{w}^*, b^*) , called respectively *weights* and *bias*, that will allow us to construct an estimator via a certain classifier

$$\mathbf{x} \mapsto \varphi \left(\frac{\mathbf{w}^{*\top} \mathbf{x}}{\sqrt{d}} + b^* \right) \quad (17)$$

to estimate the label of a new, unobserved datapoint \mathbf{x} . Here $\varphi: \mathbb{R} \rightarrow \mathcal{Y}$. In all our numerical experiments we used $\varphi(x) = \text{sign}(x)$. The choice of the parameters is performed by minimising an empirical risk function constructed via a loss function $\ell: \mathcal{Y} \times \mathbb{R} \rightarrow \mathbb{R}$ and a proper regularisation $r: \mathbb{R}^d \rightarrow \mathbb{R}$, in the form

$$\mathcal{R}(\mathbf{w}, b) \equiv \sum_{v=1}^n \ell \left(y^v, \frac{\mathbf{w}^\top \mathbf{x}^v}{\sqrt{d}} + b \right) + \lambda r(\mathbf{w}), \quad (18)$$

i.e., they are given by

$$(\mathbf{w}^*, b^*) \equiv \arg \min_{\substack{\mathbf{w} \in \mathbb{R}^d \\ b \in \mathbb{R}}} \mathcal{R}(\mathbf{w}, b). \quad (19)$$

We will assume that the loss function ℓ is convex with respect to its second argument. The parameter $\lambda \geq 0$ tunes the strength of the regularisation r , which also is assumed to be convex. The starting point of our approach is the reformulation of the task as an optimisation problem by introducing a Gibbs measure over the parameters (\mathbf{w}, b) depending on a non-negative parameter β ,

$$\mu_\beta(\mathbf{w}, b) \propto e^{-\beta \mathcal{R}(\mathbf{w}, b)} = \underbrace{e^{-\beta r(\mathbf{w})}}_{P_w(\mathbf{w})} \prod_{v=1}^n \underbrace{\exp \left[-\beta \ell \left(y^v, \frac{\mathbf{w}^\top \mathbf{x}^v}{\sqrt{d}} + b \right) \right]}_{P_y(y|\mathbf{w}, b)}, \quad (20)$$

so that, in the $\beta \rightarrow +\infty$ limit, $\mu_\beta(\mathbf{w}, b)$ concentrates on the values (\mathbf{w}^*, b^*) that minimize the empirical risk $\mathcal{R}(\mathbf{w}, b)$ and are therefore the goal of the learning process. The functions P_y and P_w can be interpreted as (unnormalised) likelihood and prior distribution respectively. Our analysis will go through the computation of the average free energy density associated with this Gibbs measure in a specific proportional limit, i.e.,

$$f_\beta := - \lim_{\substack{n, d \rightarrow +\infty \\ n/d = \alpha}} \mathbb{E}_{\mathcal{D}} \left[\frac{\ln \mathcal{Z}_\beta}{d\beta} \right] = \lim_{\substack{n, d \rightarrow +\infty \\ n/d = \alpha}} \lim_{s \rightarrow 0} \frac{\ln \mathbb{E}_{\mathcal{D}} [\mathcal{Z}_\beta^s]}{sd\beta}, \quad \mathcal{Z}_\beta := \int e^{-\beta \mathcal{R}(\mathbf{w}, b)} d\mathbf{w}. \quad (21)$$

where $\mathbb{E}_{\mathcal{D}}[\bullet]$ is the average over the training dataset. To perform the computation of such quantity, we use the so-called replica method.

A.1 Replica approach

We proceed in our calculation by assuming no prior on b , which will play a role of an extra (low-dimensional) parameter whose optimal value will be derived extremising with respect to it the final result for the free energy. We need to evaluate

$$\mathbb{E}_{\mathcal{D}} [\mathcal{Z}_\beta^s] = \prod_{a=1}^s \int d\mathbf{w}^a P_w(\mathbf{w}^a) \left(\sum_{k=\pm} \rho_k \mathbb{E}_{\mathbf{x}|k} \left[\prod_{a=1}^s P_k \left(\frac{\mathbf{w}^a \mathbf{x}}{\sqrt{d}} + b \right) \right] \right)^n. \quad (22)$$

Here and in the following, for the sake of brevity, $P_{\pm}(\eta) \equiv P_y(\pm 1|\eta)$ and similarly $\ell_{\pm}(\eta) \equiv \ell(\pm 1|\eta)$. Let us take the inner average introducing a new set of variables η^a ,

$$\begin{aligned} \mathbb{E}_{\mathbf{x}|k} \left[\prod_{a=1}^s P_k \left(\frac{\mathbf{w}^{a\top} \mathbf{x}}{\sqrt{d}} + b \right) \right] &= \prod_{a=1}^s \int d\eta^a P_k(\eta^a) \mathbb{E}_{\mathbf{x}|k} \left[\prod_{a=1}^s \delta \left(\eta^a - \frac{\mathbf{w}^{a\top} \mathbf{x}}{\sqrt{d}} + b \right) \right] \\ &= \mathbb{E}_{\Delta|k} \left[\prod_{a=1}^s \int d\eta^a P_k(\eta^a) \mathcal{N} \left(\boldsymbol{\eta} \middle| \frac{\mathbf{w}^{a\top} \boldsymbol{\mu}_k}{\sqrt{d}} - b; \frac{\Delta \mathbf{w}^a \mathbf{w}^{b\top}}{d} \right) \right], \end{aligned} \quad (23)$$

where we used the superstatistical form of the distribution of a datapoint \mathbf{x} . Using the shorthand $\mathbb{E}_{k,\Delta}[\Phi_k(\Delta)] \equiv \sum_{k=\pm} \rho_k \int_0^\infty \varrho(\Delta) \Phi_k(\Delta) d\Delta$, we can write then

$$\begin{aligned} \mathbb{E}_{\mathcal{D}} [Z_{\beta}^s] &= \prod_{a=1}^s \int d\mathbf{w}^a P_w(\mathbf{w}^a) \left(\mathbb{E}_{k,\Delta} \left[\prod_{a=1}^s \int d\eta^a P_k(\eta^a) \mathcal{N} \left(\boldsymbol{\eta}; \frac{\mathbf{w}^{a\top} \boldsymbol{\mu}_k}{d} + b; \frac{\Delta \mathbf{w}^a \mathbf{w}^{b\top}}{d} \right) \right] \right)^n \\ &= \left(\prod_{a \leq b} \iint \mathcal{D} Q^{ab} \mathcal{D} \hat{Q}^{ab} \right) \left(\prod_a \mathcal{D} m^a \mathcal{D} \hat{m}^a \right) e^{-d\beta\Phi^{(s)}}. \end{aligned} \quad (24)$$

In the equation above we introduced the *order parameters*

$$Q_{\Delta}^{ab} = \Delta \frac{\mathbf{w}^{a\top} \mathbf{w}^b}{d} \in \mathbb{R}, \quad a, b = 1, \dots, s, \quad (25)$$

$$m_k^a = \frac{\mathbf{w}^{a\top} \boldsymbol{\mu}_k}{\sqrt{d}} \in \mathbb{R}, \quad a = 1, \dots, s, \quad (26)$$

whilst $\iint \mathcal{D} Q^{ab} \mathcal{D} \hat{Q}^{ab}$ express the integration over Q_{Δ}^{ab} and \hat{Q}_{Δ}^{ab} , to be intended as functions of Δ . Similarly, $\mathcal{D} m^a \mathcal{D} \hat{m}^a \propto \prod_{k=\pm} dm_k^a d\hat{m}_k^a$. We have also introduced the replicated free-energy

$$\begin{aligned} \beta\Phi^{(s)}(Q, M, \hat{Q}, \hat{m}, b) &= \sum_{k=\pm} \sum_a \hat{m}_k^{a\top} m_k^a + \sum_{a \leq b} \mathbb{E}_{\Delta} [\hat{Q}_{\Delta}^{ab} Q_{\Delta}^{ab}] \\ &\quad - \frac{1}{d} \ln \prod_{a=1}^s \int P_w(\mathbf{w}^a) d\mathbf{w}^a \left(\prod_{a \leq b} e^{\mathbb{E}_{\Delta} [\Delta \hat{Q}_{\Delta}^{ab}] \mathbf{w}^{a\top} \mathbf{w}^b} \prod_a e^{\sqrt{d} \sum_k \hat{m}_k^a \mathbf{w}^{a\top} \boldsymbol{\mu}_k} \right) \\ &\quad - \alpha \ln \mathbb{E}_{k,\Delta} \left[\prod_{a=1}^s \int d\eta^a P_k(\eta^a) \mathcal{N} \left(\boldsymbol{\eta} \middle| m_k^a + b, Q_{\Delta}^{ab} \right) \right]. \end{aligned} \quad (27)$$

At this point, the free energy f_{β} should be computed functionally extremizing with respect to all the order parameters by virtue of the Laplace approximation (in addition to b),

$$f_{\beta} = \lim_{s \rightarrow 0} \text{Extr}_{\substack{m, \hat{m} \\ Q, \hat{Q}, b}} \frac{\Phi^{(s)}(Q, m, \hat{Q}, \hat{m}, b)}{s}. \quad (28)$$

However, the convexity of the problem allows us to make an important simplification.

Replica symmetric ansatz Before taking the $s \rightarrow 0$ limit we make the replica symmetric assumptions

$$\begin{aligned} Q_{\Delta}^{aa} &= \begin{cases} R_{\Delta}, & a = b \\ Q_{\Delta}, & a \neq b \end{cases} & \hat{Q}_{\Delta}^{aa} &= \begin{cases} -\frac{1}{2} \hat{R}_{\Delta}, & a = b \\ \hat{Q}_{\Delta}, & a \neq b \end{cases} \\ m_k^a &= m_k & \hat{m}_k^a &= \hat{m}_k \quad \forall a \end{aligned} \quad (29)$$

By means of the replica symmetric hypothesis, we can write

$$Q_{\Delta}^{ab} \mapsto \mathbf{Q}_{\Delta} \equiv (R_{\Delta} - Q_{\Delta}) \mathbf{I}_{s,s} + Q_{\Delta} \mathbf{1}_s. \quad (30)$$

The inverse matrix is therefore

$$\mathbf{Q}_{\Delta}^{-1} = \frac{1}{R_{\Delta} - Q_{\Delta}} \mathbf{1}_s - \frac{Q_{\Delta}}{(R_{\Delta} - Q_{\Delta} + sQ_{\Delta})(R_{\Delta} - Q_{\Delta})} \mathbf{I}_{s,s}, \quad (31)$$

whereas

$$\det \mathbf{Q}_\Delta = (R_\Delta - Q_\Delta)^{s-1} (R_\Delta - Q_\Delta + sQ_\Delta) = 1 + s \ln(R_\Delta - Q_\Delta) + s \frac{Q_\Delta}{R_\Delta - Q_\Delta} + o(s). \quad (32)$$

If we denote $V_\Delta := R_\Delta - Q_\Delta$

$$\ln \mathbb{E}_{k,\Delta} \left[\prod_{a=1}^s \int d\eta^a P_k(\eta^a) \mathcal{N}(\boldsymbol{\eta} | m_k^a + b, Q_\Delta^{ab}) \right] = s \mathbb{E}_{k,\Delta,\zeta} \left[\ln Z_k(m_k + b + \sqrt{Q_\Delta} \zeta, V_\Delta) \right] + o(s), \quad (33)$$

with $\zeta \sim \mathcal{N}(0, 1)$ normally distributed random variable. In the expression above, we have also introduced the function

$$Z_k(m, V) := \int \frac{d\eta P_k(\eta)}{\sqrt{2\pi V}} e^{-\frac{(\eta-m)^2}{2V}}. \quad (34)$$

On the other hand, denoting by $\hat{V}_\Delta = \hat{R}_\Delta + \hat{Q}_\Delta$,

$$\begin{aligned} & \frac{1}{d} \ln \prod_{a=1}^s \left(\int d\mathbf{w}^a P_w(\mathbf{w}^a) e^{-\mathbb{E}_\Delta[\Delta \hat{V}_\Delta] \frac{\|\mathbf{w}^a\|^2}{2} + \sqrt{d} \sum_k \hat{m}_k \mathbf{w}^{a\top} \boldsymbol{\mu}_k} \prod_b e^{\frac{1}{2} \mathbb{E}_\Delta[\Delta \hat{Q}_\Delta] \mathbf{w}^{a\top} \mathbf{w}^b} \right) = \\ & = \frac{s}{d} \mathbb{E}_\xi \ln \left[\int d\mathbf{w} P_w(\mathbf{w}) \exp \left(-\mathbb{E}_\Delta[\Delta \hat{V}_\Delta] \frac{\|\mathbf{w}\|^2}{2} + \sqrt{d} \sum_k \hat{m}_k \mathbf{w}^\top \boldsymbol{\mu}_k + \sqrt{\mathbb{E}_\Delta[\Delta \hat{Q}_\Delta]} \boldsymbol{\xi}^\top \mathbf{w} \right) \right] + o(s). \end{aligned} \quad (35)$$

In the expression above we have introduced $\boldsymbol{\xi} \sim \mathcal{N}(\mathbf{0}, \mathbf{I}_d)$ and denote the average over it by $\mathbb{E}_\xi[\bullet]$. Therefore, the (replicated) *replica symmetric* free-energy is given by

$$\lim_{s \rightarrow 0} \frac{\beta}{s} \Phi_{\text{RS}}^{(s)} = \sum_{k=\pm} \hat{m}_k m_k + \frac{\mathbb{E}_\Delta [\hat{V}_\Delta Q_\Delta - \hat{Q}_\Delta V_\Delta - \hat{V}_\Delta V_\Delta]}{2} - \alpha \beta \Psi_{\text{out}}(m, Q, V) - \beta \Psi_w(\hat{m}, \hat{Q}, \hat{V}) \quad (36)$$

where we have defined two contributions

$$\begin{aligned} \Psi_{\text{out}}(m, Q, V) &:= \beta^{-1} \mathbb{E}_{k,\Delta,\xi} [\ln Z_k(\omega_k, V_\Delta)] \\ \Psi_w(\hat{m}, \hat{Q}, \hat{V}) &:= \frac{1}{\beta d} \mathbb{E}_\xi \ln \left[\int P_w(\mathbf{w}) d\mathbf{w} \exp \left(-\frac{\mathbb{E}_\Delta[\Delta \hat{V}_\Delta] \|\mathbf{w}\|^2}{2} + \sqrt{d} \sum_k \hat{m}_k \mathbf{w}^\top \boldsymbol{\mu}_k + \sqrt{\mathbb{E}_\Delta[\Delta \hat{Q}_\Delta]} \boldsymbol{\xi}^\top \mathbf{w} \right) \right] \end{aligned} \quad (37)$$

and introduced, for future convenience,

$$\omega_k := m_k + b + \sqrt{Q_\Delta} \zeta. \quad (38)$$

Note that we have separated the contribution coming from the chosen loss (the so-called *channel* part Ψ_{out}) from the contribution depending on the regularisation (the *prior* part Ψ_w). To write down the saddle-point equations in the $\beta \rightarrow +\infty$ limit, let us first rescale our order parameters as $\hat{m}_k \mapsto \beta \hat{m}_k$, $\hat{Q}_\Delta \mapsto \beta^2 \hat{Q}_\Delta$, $\hat{V} \mapsto \beta \hat{V}$ and $V_\Delta \mapsto \beta^{-1} V_\Delta$. For $\beta \rightarrow +\infty$ the channel part is

$$\Psi_{\text{out}}(m, Q, V) = -\mathbb{E}_{k,\Delta,\zeta} \left[\frac{(h_k - \omega_k)^2}{2V_\Delta} + \ell_k(h_k) \right]. \quad (39)$$

where we have written Ψ_{out} in terms of a proximal

$$\arg \min_u \left[\frac{(u - \omega_k)^2}{2V_\Delta} + \ell_k(u) \right]. \quad (40)$$

A similar expression can be obtained for Ψ_w . Introducing the proximal

$$\mathbf{g} = \arg \min_{\mathbf{w}} \left(\frac{\mathbb{E}_\Delta[\Delta \hat{V}_\Delta] \|\mathbf{w}\|^2}{2} - \sqrt{d} \sum_k \hat{m}_k \mathbf{w}^\top \boldsymbol{\mu}_k - \sqrt{\mathbb{E}_\Delta[\Delta \hat{Q}_\Delta]} \boldsymbol{\xi}^\top \mathbf{w} + \lambda r(\mathbf{w}) \right) \in \mathbb{R}^d \quad (41)$$

We can rewrite the prior contribution Ψ_w as

$$\Psi_w(\hat{m}, \hat{Q}, \hat{V}) = -\frac{1}{d} \mathbb{E}_\xi \left[\frac{\mathbb{E}_\Delta[\Delta \hat{V}_\Delta] \|\mathbf{g}\|^2}{2} - \sqrt{d} \sum_k \hat{m}_k \mathbf{g}^\top \boldsymbol{\mu}_k - \sqrt{\mathbb{E}_\Delta[\Delta \hat{Q}_\Delta]} \boldsymbol{\xi}^\top \mathbf{g} + \lambda r(\mathbf{g}) \right] \quad (42)$$

The analogy between the two contributions is evident, aside from the different dimensionality of the involved objects. The replica symmetric free energy (21) in the $\beta \rightarrow +\infty$ limit is computed by extremising with respect to the introduced order parameters,

$$f_{\text{RS}} = \text{Extr}_{\substack{m, Q, V, b \\ \hat{m}, \hat{Q}, \hat{V}}} \left[\sum_{k=\pm} \hat{m}_k m_k + \frac{\mathbb{E}_{\Delta} [\hat{V}_{\Delta} Q_{\Delta} - \hat{Q}_{\Delta} V_{\Delta} - \hat{V}_{\Delta} V_{\Delta}]}{2} - \alpha \Psi_{\text{out}}(m, Q, V) - \Psi_w(\hat{m}, \hat{Q}, \hat{V}) \right]. \quad (43)$$

To do so, we have to write down a set of saddle-point equations and solve them.

Saddle-point equations The saddle-point equations are derived straightforwardly from the obtained free energy functionally extremising with respect to all parameters. A first set of equations is obtained from Ψ_{out} . Introducing

$$f_k \equiv \frac{h_k - \omega_k}{V_{\Delta}} \quad (44)$$

(and keeping in mind that this quantity is also Δ -dependent) we have

$$\hat{Q}_{\Delta} = \alpha \mathbb{E}_{k, \zeta} [f_k^2], \quad \hat{V}_{\Delta} = -\frac{\alpha \mathbb{E}_{k, \zeta} [f_k \zeta]}{\sqrt{Q_{\Delta}}}, \quad \hat{m}_k = \alpha \rho_k \mathbb{E}_{\Delta, \zeta} [f_k], \quad b = \mathbb{E}_{k, \Delta, \zeta} [h_k - m_k]. \quad (45)$$

Denoting $\hat{q} := \mathbb{E}[\Delta \hat{Q}_{\Delta}]$ and $\hat{v} := \mathbb{E}[\Delta \hat{V}_{\Delta}]$, the saddle-point equations from Ψ_w are

$$V_{\Delta} = \frac{1}{d} \frac{\Delta \mathbb{E}_{\xi} [\mathbf{g}^{\top} \xi]}{\sqrt{\hat{q}}} \quad Q_{\Delta} = \frac{\Delta}{d} \mathbb{E}_{\xi} [\|\mathbf{g}\|^2] \quad m_k = \frac{1}{\sqrt{d}} \mathbb{E}_{\xi} [\mathbf{g}^{\top} \mu_k]. \quad (46)$$

Observe that the equations above imply that $V_{\Delta} = v\Delta$ and $Q_{\Delta} = q\Delta$, where v and q are some constant that do not depend on Δ ¹. We can rewrite

$$v = \frac{\mathbb{E}_{\xi} [\mathbf{g}^{\top} \xi]}{d \sqrt{\hat{q}}} \quad q = \frac{\mathbb{E}_{\xi} [\|\mathbf{g}\|^2]}{d} \quad m_k = \frac{\mathbb{E}_{\xi} [\mathbf{g}^{\top} \mu_k]}{\sqrt{d}} \quad (47)$$

and the remaining equations as

$$\hat{q} = \alpha \mathbb{E}_{k, \zeta, \Delta} [\Delta f_k^2], \quad \hat{v} = -\frac{\alpha}{\sqrt{q}} \mathbb{E}_{k, \Delta, \zeta} [\sqrt{\Delta} f_k \zeta], \quad \hat{m}_k = \alpha \rho_k \mathbb{E}_{\Delta, \zeta} [f_k], \quad b = \mathbb{E}_{k, \Delta, \zeta} [h_k - m_k]. \quad (48)$$

To obtain the replica symmetric free energy, therefore, the given set of equation has to be solved, and the result then plugged in Eq. (43).

A.2 Training and test errors

The order parameters introduced to solve the problem allow us to reach our ultimate goal of computing the average errors of the learning process. We will start with the estimation of the training loss

$$\epsilon_{\ell} \equiv \frac{1}{n} \sum_{\nu=1}^n \ell \left(y^{\nu}, \frac{\mathbf{w}^{\star} \mathbf{x}^{\nu}}{\sqrt{d}} + b^{\star} \right) \quad (49)$$

in the $n \rightarrow +\infty$ limit. The complication in computing this quantity is that the order parameters found in the learning process are, of course, correlated with the dataset \mathcal{D} used for the learning itself. The best way to proceed is to observe that

$$\mathbb{E}_{\mathcal{D}} [\mathcal{R}(\mathbf{w}^{\star}, b^{\star})] = -\lim_{\beta \rightarrow +\infty} \mathbb{E}_{\mathcal{D}} [\partial_{\beta} \ln \mathcal{Z}_{\beta}] = \lambda \mathbb{E}_{\mathcal{D}} [r(\mathbf{w}^{\star})] + \epsilon_{\ell}$$

where

$$\epsilon_{\ell} = -\lim_{\beta \rightarrow +\infty} \partial_{\beta} (\beta \Psi_{\text{out}}) = \lim_{\beta \rightarrow +\infty} \mathbb{E}_{k, \Delta, \zeta} \left[\int \frac{\ell_k(\eta) e^{-\frac{\beta(\eta - m_k^{\star})^2}{2\Delta v^{\star}} - \beta \ell_k(\eta)}}{\sqrt{2\pi\beta^{-1}v^{\star}\Delta} Z_k(\omega_k^{\star}, \beta^{-1}v^{\star}\Delta)} d\eta \right]. \quad (50)$$

¹This was largely expected in our setting, but we preferred to keep a redundant derivation as this factorisation cannot be performed when the derivation is generalised to the case of random covariance matrices which are not multiple of the identity.

In the $\beta \rightarrow +\infty$ limit, the integral concentrates on the minimiser of the exponent, that is, by definition, the proximal h_k . In conclusion,

$$\epsilon_\ell = \mathbb{E}_{k,\Delta,\xi}[\ell_k(h_k)]. \quad (51a)$$

By means of the same concentration result, the training error is

$$\epsilon_t = \frac{1}{n} \sum_{\nu=1}^n \mathbb{I} \left(\varphi \left(\frac{\mathbf{w}^{\star\top} \mathbf{x}^\nu}{\sqrt{d}} + b^\star \right) \neq y^\nu \right) \xrightarrow{n \rightarrow +\infty} \mathbb{E}_{k,\Delta,\zeta} [\mathbb{I}(\varphi(h_k) \neq y_k)]. \quad (51b)$$

The expressions above hold in general, but, as anticipated, important simplifications can occur in the set of saddle-point equations (48) and (58) depending on the choice of the loss ℓ and of the regularisation function r . The generalisation (or test) error can be written instead as

$$\epsilon_g = \mathbb{E}_{(y^{\text{new}}, \mathbf{x}^{\text{new}})} \left[\mathbb{I} \left(\varphi \left(\frac{\mathbf{w}^{\star\top} \mathbf{x}^{\text{new}}}{\sqrt{d}} + b^\star \right) \neq y^{\text{new}} \right) \right]. \quad (51c)$$

This expression can be rewritten as

$$\begin{aligned} \epsilon_g &= \mathbb{E}_k \left[\int \mathbb{I}(\varphi(\eta) = y_k) \mathbb{E}_{\mathbf{x}^{\text{new}}} \left[\delta \left(\eta - \frac{\mathbf{w}^{\star\top} \mathbf{x}^{\text{new}}}{\sqrt{d}} - b^\star \right) \right] d\eta \right] \\ &= \mathbb{E}_{k,\Delta} \left[\int \mathbb{I}(\varphi(\eta) = y_k) \mathbb{E}_{\mathbf{x}^{\text{new}}|\Delta} \left[\delta \left(\eta - \frac{\mathbf{w}^{\star\top} \mathbf{x}^{\text{new}}}{\sqrt{d}} - b^\star \right) \right] d\eta \right] \\ &\xrightarrow{d \rightarrow +\infty} \mathbb{E}_{k,\Delta} \left[\int \mathbb{I}(\varphi(\eta) = y_k) \mathcal{N}(\eta | m_k^\star + b^\star, \Delta q^\star) d\eta \right] \\ &= \mathbb{E}_{k,\Delta,\zeta} \left[\mathbb{I} \left(\varphi \left(m_k^\star + \sqrt{\Delta q^\star} \zeta + b^\star \right) \neq y_k \right) \right]. \end{aligned} \quad (51d)$$

This can be easily computed numerically once the order parameters (including their functional dependence on Δ) are given.

A.3 Ridge regularisation

Let us fix now $r(\mathbf{w}) = \frac{1}{2} \|\mathbf{w}\|^2$. In this case, the computation of Ψ_w can be performed explicitly via a Gaussian integration, and the saddle-point equations can take a more compact form that is particularly suitable for a numerical solution. In particular

$$\mathbf{g} = \frac{\sqrt{d} \sum_k \hat{m}_k \boldsymbol{\mu}_k + \sqrt{\hat{q}} \boldsymbol{\xi}}{\lambda + \hat{\nu}} \quad (52)$$

so that the prior saddle-point equations obtained from Ψ_w become

$$\nu = \frac{1}{\lambda + \hat{\nu}} \quad (53a)$$

$$q = \frac{\sum_{kk'} \hat{m}_k \hat{m}_{k'} \boldsymbol{\mu}_k^\top \boldsymbol{\mu}_{k'} + \hat{q}}{(\lambda + \hat{\nu})^2} \quad (53b)$$

$$m_k = \frac{\sum_{k'} \hat{m}_{k'} \boldsymbol{\mu}_{k'}^\top \boldsymbol{\mu}_k}{\lambda + \hat{\nu}}. \quad (53c)$$

Quadratic loss If we consider a quadratic loss $\ell(y, x) = \frac{1}{2} (y - x)^2$, then an explicit formula for the proximal can be found, namely

$$f_k = \frac{y_k - \omega_k}{1 + \nu \Delta} \quad (54)$$

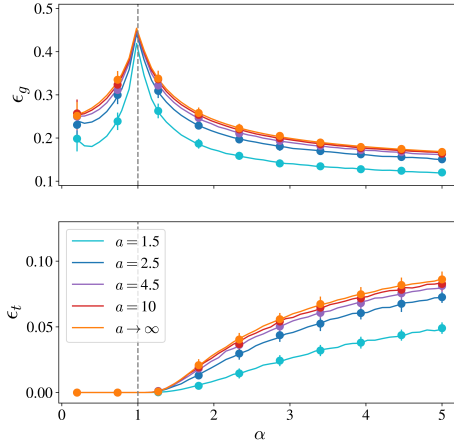


Figure 7: Test error ϵ_g (top) and training error ϵ_t (bottom) as predicted by Eq. (8) in the unbalanced $\rho = 1/4$ case. The dataset distribution is parametrised as in Eq. (11). The classification task is solved using a quadratic loss with ridge regularisation with $\lambda = 10^{-5}$. Dots correspond to the average outcome of 50 numerical experiments in dimension $d = 10^3$. In our parametrisation, the population covariance is $\boldsymbol{\Sigma} = \mathbf{I}_d$ for all values of a and moreover, for $a \rightarrow +\infty$, the case of pure Gaussian clouds $P(\mathbf{x}|\boldsymbol{\mu}) = \mathcal{N}(\mathbf{x}|\boldsymbol{\mu}, \mathbf{I}_d)$ is recovered.

so that the second set of saddle-point equations (48) can be written as

$$\hat{q} = \alpha \mathbb{E}_{k,\Delta} \left[\frac{\Delta(y_k - m_k - b)^2}{(1 + v\Delta)^2} \right] + \alpha q \mathbb{E}_\Delta \left[\frac{\Delta^2}{(1 + v\Delta)^2} \right], \quad (55a)$$

$$\hat{v} = \alpha \mathbb{E}_\Delta \left[\frac{\Delta}{1 + v\Delta} \right] = \frac{1 - v\lambda}{v}, \quad (55b)$$

$$\hat{m}_k = \alpha \rho_k (y_k - m_k - b) \mathbb{E}_\Delta \left[\frac{1}{1 + v\Delta} \right]. \quad (55c)$$

so that v satisfies the self-consistent equation

$$\frac{1 - v\lambda}{v\alpha} = \mathbb{E}_\Delta \left[\frac{\Delta}{1 + v\Delta} \right]. \quad (56)$$

As a complement to the information given in the main text, in Fig. 7 we give some numerical results for the case of *unbalanced* clusters, which show a perfect agreement between the theoretical predictions and the numeral results.

Logistic loss We consider now the relevant case of the logistic loss $\ell(x) = \ln(1 + e^{-x})$. The proximal equation for this loss is the solution of the equations:

$$f_k = \arg \min_u \left[\frac{\Delta v u^2}{2} + \ln \left(1 + e^{-(\Delta v u + \omega_k)} \right) \right] \quad (57)$$

having only one solution for which, however, there is no closed-form expression; the equation can be solved numerically. To consider the $\lambda \rightarrow 0$ limit, it is convenient rescaling $\hat{v} \mapsto \lambda \hat{v}$, $v \mapsto \lambda^{-1} v$, $m \mapsto \lambda^{-1} m$, and $q \mapsto \lambda^{-2} q$. The prior equations become in this case

$$v = \frac{1}{1 + \hat{v}} \quad (58a)$$

$$q = \frac{\sum_{kk'} \hat{m}_k \hat{m}_{k'} \boldsymbol{\mu}_k^\top \boldsymbol{\mu}_{k'} + \hat{q}}{(1 + \hat{v})^2} \quad (58b)$$

$$m_k = \frac{\sum_{k'} \hat{m}_{k'} \boldsymbol{\mu}_{k'}^\top \boldsymbol{\mu}_k}{1 + \hat{v}}, \quad (58c)$$

so that they have no dependence on λ left. The channel part, instead, keeps the form in (48), but with proximal

$$f_k = \arg \min_u \left[\frac{\Delta v u^2}{2} + \lambda \ln \left(1 + e^{-\frac{\Delta v u + \omega_k}{\lambda}} \right) \right]. \quad (59)$$

Note that for $\lambda \rightarrow 0$, minimising the cross-entropy loss yields precisely the max-margin estimator [49].

A.4 The uncorrelated-teacher case and universality

In a recent paper, Gerace et al. [17] showed that a classification task on Gaussian clouds exhibits universality features in the case in which the labels are randomly assigned to the dataset points. Under the hypothesis of a loss function satisfying $\ell(y, \eta) = \ell(-y, -\eta)$ with ridge regularisation, they show that a dataset obtained from a mixture of Gaussian clouds with equal covariance $\boldsymbol{\Sigma}$ is equivalent to a dataset obtained from a single Gaussian cloud with zero mean and covariance $\boldsymbol{\Sigma}$. Moreover, using ridge regression, the training loss ϵ_ℓ is shown to depend on the sample complexity only (and not on $\boldsymbol{\Sigma}$) in the $\lambda \rightarrow 0^+$ limit. This result has been generalised immediately afterwards by Pesce et al. [46], who showed that the same picture holds in the case in which labels are generated by a ‘‘teacher’’ modeled by a distribution $P_0(y|\tau)$, with $P_0(y|\tau) = P_0(-y|-\tau)$, and parametrised by vector $\boldsymbol{\theta}_0 \in \mathbb{R}^d$, which is *uncorrelated* with the data structure.

In our setting, this would amount to considering a database \mathcal{D} generated from the joint distribution

$$P(\mathbf{x}, y) = P_0 \left(y \middle| \frac{\boldsymbol{\theta}_0^\top \mathbf{x}}{\sqrt{d}} \right) \sum_{k=\pm} \rho_k \mathbb{E}[\mathcal{N}(\mathbf{x} | \boldsymbol{\mu}_k, \Delta \mathbf{I}_d)], \quad (60)$$

the random labels case corresponding to $P_0(y|\tau)$ given by a Rademacher distribution in y independent of τ . The condition of uncorrelated teacher is expressed by²

$$\lim_{d \rightarrow +\infty} \frac{\boldsymbol{\theta}_0^\top \boldsymbol{\mu}_\pm}{d} = 0. \quad (61)$$

Let us assume for simplicity that we adopt ridge regularisation, $r(\mathbf{w}) = \frac{\lambda}{2} \|\mathbf{w}\|^2$. The analysis of this setting is perfectly analogous to the one discussed above, but provides slightly different fixed-point equations for the order parameters, and in particular, it requires introducing the overlap between the weights \mathbf{w} and the teacher parameter $\boldsymbol{\theta}_0$, $t = \frac{1}{d} \mathbf{w}^\top \boldsymbol{\theta}_0$, and its corresponding Lagrange multiplier \hat{t} . Following therefore a procedure that combines the one presented above and the derivation given in Ref. [46] for the Gaussian case, we can obtain the following fixed-point equations,

$$\begin{cases} v = \frac{1}{\lambda + \hat{v}} \\ q = \frac{\gamma \hat{t}^2 + \|\sum_c \hat{m}_c \boldsymbol{\mu}_c\|^2 + q}{(\lambda + \hat{v})^2}, \\ m_\pm = \frac{\sum_c \hat{m}_c \boldsymbol{\mu}_c^\top \boldsymbol{\mu}_\pm}{\lambda + \hat{v}}, \\ t = \frac{\gamma \hat{t}}{\lambda + \hat{v}} \end{cases} \quad \begin{cases} \hat{q} = \alpha \sum_y \mathbb{E}_{\pm, \Delta, \zeta} \left[\Delta Z_0 \left(y, \sqrt{\frac{\Delta}{q}} t \zeta, \Delta \gamma - \Delta \frac{t^2}{q} \right) f^2(y, \omega_\pm, v) \right], \\ \hat{v} = -\alpha \sum_y \mathbb{E}_{\pm, \Delta, \zeta} \left[Z_0 \left(y, \sqrt{\frac{\Delta}{q}} t \zeta, \Delta \gamma - \Delta \frac{t^2}{q} \right) \partial_\omega f(y, \omega_\pm, v) \right], \\ \hat{m}_\pm = \alpha \rho_\pm \sum_y \mathbb{E}_{\Delta, \zeta} \left[Z_0 \left(y, \sqrt{\frac{\Delta}{q}} t \zeta, \Delta \gamma - \Delta \frac{t^2}{q} \right) f_\pm(y, \omega_\pm, v) \right] \\ \hat{t} = \alpha \sum_y \mathbb{E}_{\pm, \Delta, \zeta} \left[\partial_\omega Z_0 \left(y, \sqrt{\frac{\Delta}{q}} t \zeta, \Delta \gamma - \Delta \frac{t^2}{q} \right) \Delta f(y, \omega_\pm, v) \right], \end{cases} \quad (62)$$

with $\gamma := \frac{1}{d} \|\boldsymbol{\theta}_0\|^2$ and

$$\begin{aligned} f(y, \omega, v) &:= \arg \min_u \left[\frac{\Delta v u^2}{2} + \ell(y, \omega + v \Delta u) \right], \quad \omega_\pm := b + m_\pm + \sqrt{\Delta q} \zeta \\ b &= \sum_y \mathbb{E}_{\pm, \Delta, \zeta} \left[Z_0 \left(y, \sqrt{\frac{\Delta}{q}} t \zeta, \Delta \rho - \Delta \frac{t^2}{q} \right) (\omega_\pm + v \Delta f(y, \omega_\pm, v) - m_\pm) \right]. \end{aligned} \quad (63)$$

that provide us the quantities to plug into Eqs. (51) to compute the asymptotic errors. In the equations above, $Z_0(y, \omega, v) := \mathbb{E}_z [P_0(y|\omega + \sqrt{v}z)]$ with $z \sim \mathcal{N}(0, 1)$.

Mean universality Following Ref. [46], let us now make the additional assumption $P_0(y|\tau) = P_0(-y|-\tau)$. This implies that $Z_0(y, \omega, v) = Z_0(-y, -\omega, v)$. In this case, we claim that the solution has $m_\pm = \hat{m}_\pm = b = 0$. It is clear that if $\hat{m}_\pm = 0$, then $m_\pm = 0$ and, moreover, because of parity, the solution $b = 0$ is consistent. On the other hand, if $m_\pm = 0$ and $b = 0$, remembering that $\ell(y, \eta) = \ell(-y, -\eta)$, then $f(1, \omega, v) = -f(-1, -\omega, v)$ so that the formula for \hat{m}_\pm involves a Gaussian integral of an odd function which is, therefore, zero, implying $\hat{m}_\pm = 0$. We are left therefore with a much simpler set of fixed-point equations, namely

$$\begin{cases} v = \frac{1}{\lambda + \hat{v}} \\ q = \frac{\gamma \hat{t}^2 + q}{(\lambda + \hat{v})^2}, \\ t = \frac{\gamma \hat{t}}{\lambda + \hat{v}} \end{cases} \quad \begin{cases} \hat{q} = \alpha \sum_y \mathbb{E}_{\Delta, \zeta} \left[\Delta Z_0 \left(y, \sqrt{\frac{\Delta}{q}} t \zeta, \Delta \gamma - \Delta \frac{t^2}{q} \right) f^2(y, \omega, v) \right], \\ \hat{v} = -\alpha \sum_y \mathbb{E}_{\Delta, \zeta} \left[Z_0 \left(y, \sqrt{\frac{\Delta}{q}} t \zeta, \Delta \gamma - \Delta \frac{t^2}{q} \right) \partial_\omega f(y, \omega, v) \right], \\ \hat{t} = \alpha \sum_y \mathbb{E}_{\Delta, \zeta} \left[\partial_\omega Z_0 \left(y, \sqrt{\frac{\Delta}{q}} t \zeta, \Delta \gamma - \Delta \frac{t^2}{q} \right) \Delta f(y, \omega, v) \right], \end{cases} \quad (64)$$

with

$$f(y, \omega, v) := \arg \min_u \left[\frac{\Delta v u^2}{2} + \ell(y, \omega + v \Delta u) \right], \quad \omega := \sqrt{\Delta q} \zeta, \quad (65)$$

which is exactly the formula we would have obtained assuming $\boldsymbol{\mu}_\pm = \mathbf{0}$, i.e., the presence of *one cloud only*, so that $P(\mathbf{x}, y) = P_0(y|\frac{1}{\sqrt{d}} \boldsymbol{\theta}_0^\top \mathbf{x}) \mathbb{E}[\mathcal{N}(\mathbf{x}|\mathbf{0}, \Delta \mathbf{I}_d)]$. This *mean universality* result generalises the result in Ref. [46] for Gaussian clouds.

Random labels under square loss The case of *random label* is particularly interesting as it exhibits further universality when the square loss is adopted. In this case, $P_0(y|\tau)$ is simply the Rademacher distribution. Using $\ell(y, \eta) = \frac{1}{2}(y - \eta)^2$, the equations greatly simplify and we obtain

$$\begin{cases} v = \frac{1}{\lambda + \hat{v}}, \\ q = \frac{\hat{q}}{(\lambda + \hat{v})^2}, \end{cases} \quad \begin{cases} \hat{q} = \alpha \mathbb{E}_\Delta \left[\frac{\Delta + q \Delta^2}{(1 + v \Delta)^2} \right], \\ \hat{v} = \alpha \mathbb{E}_\Delta \left[\frac{\Delta}{1 + v \Delta} \right], \end{cases} \quad (66)$$

²In our case, this condition is simpler than in Ref. [46] as we assume that each class has the same homogeneous covariance.

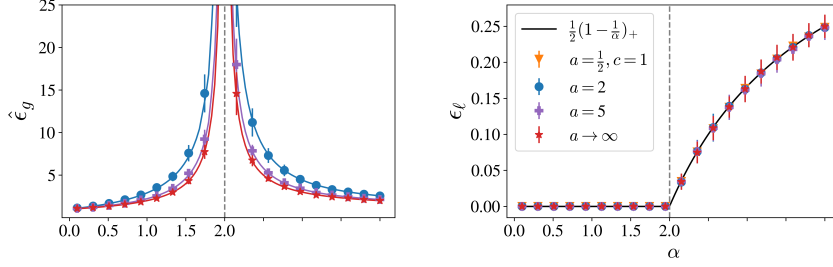


Figure 8: Test loss $\hat{\epsilon}_g$ (**left**) and training loss ϵ_ℓ (**right**) obtained by running numerical experiments for a classification task on *two* clouds with opposite means and randomly labeled points. Each cloud is generated with distribution in Eq. (10b) for different values of a (i.e., different power-law decay). All clouds with $a > 1$ have the same covariance $\Sigma = \mathbf{I}_d$ and are obtained using Eq. (11). The case $a = 1/2$ and $c = 1$, instead, corresponds to infinite σ^2 (note that in this case $\hat{\epsilon}_g$ is infinite and is therefore not plotted). For each a , the numerical experiments are compared with the theoretical prediction for a random label classification task on a single cloud centered in the origin and with the same parameter a , showing an excellent agreement. Note that the training loss is found to be universal and following (70), independently from the variance distribution.

whereas $t = \hat{t} = 0$, so that the test loss, obtained by using $\varphi(y, \eta) = (y - \eta)^2$, and the training loss are

$$\hat{\epsilon}_g := \mathbb{E}_{(y,x)} \left[\left(y - \frac{1}{\sqrt{d}} \mathbf{x}^\top \mathbf{w}^\star \right)^2 \right] = 1 + \sigma^2 q, \quad \epsilon_\ell = \frac{1}{2} \mathbb{E}_\Delta \left[\frac{1 + q\Delta}{(1 + v\Delta)^2} \right]. \quad (67)$$

Note that the test loss is infinite if $\sigma^2 = +\infty$. Introducing the notation $\delta_k := \mathbb{E}[(1 + v\Delta)^{-k}]$, the fixed-point equations above read

$$\begin{cases} v = \frac{1}{\lambda + \hat{v}}, \\ q = \frac{\hat{q}}{(\lambda + \hat{v})^2}, \end{cases} \quad \begin{cases} \hat{q} = \alpha \frac{\delta_1 - \delta_2}{v} + \alpha q \frac{1 - 2\delta_1 + \delta_2}{v^2}, \\ \hat{v} = \alpha \frac{1 - \delta_1}{v}, \end{cases}, \quad \epsilon_\ell = \frac{1}{2} \left(\delta_2 + q \frac{\delta_1 - \delta_2}{v} \right). \quad (68)$$

Observe now that in the limit $\lambda \rightarrow 0$

$$x := \frac{q}{v} = \frac{\hat{q}}{\hat{v}} = -\frac{\delta_2 - 2\delta_1 + 1}{\delta_1 - 1} x + \frac{\delta_2 - \delta_1}{\delta_1 - 1}, \quad (69)$$

which is solved by $x = 1$, so that in this limit $\epsilon_\ell = \delta_1$. But, on the other hand, the fixed point equation for \hat{v} implies that v is such that $\delta_1 = 1 - 1/\alpha$ if $\alpha \geq 1$, and zero otherwise (as $\delta_1 \geq 0$ by definition) so that we recover the universal formula for the training loss obtained by Gerace et al. [17],

$$\epsilon_\ell = \frac{1}{2} \left(1 - \frac{1}{\alpha} \right)_+, \quad (70)$$

where $(x)_+ = x\theta(x)$. Note that this formula *does not depend on the choice of the distribution of Δ* . We verify this result in Fig. 8. We run numerical experiments using a quadratic loss on datapoints split in two clouds of equal weights centered around $\mu_1 = -\mu_2 \sim \mathcal{N}(\mathbf{0}, \mathbf{I}_d)$, and generated with distribution as in (11), parametrised by a , so that each cloud has $\Sigma = \mathbf{I}_d$. Labels are assigned randomly with Rademacher distribution. The results are compared with the prediction for *one* cloud with $\mu = \mathbf{0}$ but with the same parameter a . We see that mean-independence in this setting is indeed verified.

B Note on the numerical results

State evolution equations Each average appearing in the update of the order parameters was performed using 10^5 instances of the variance. For the convergence criterion, we use a tolerance of 10^{-5} ; the algorithm stops and returns the parameters after at most 10^3 updates.

Note that, in the case of logistic regression, there are numerical instabilities when computing \hat{v} . To avoid them we first notice that $f_k + \partial_\eta \ell_k(\Delta v f_k + \omega_k) = 0$ holds, and we use this to compute $\partial_\omega f_k$ which we use in the application of Stein's lemma, rewriting the equation as

$$\hat{v} = -\frac{\alpha \mathbb{E}_{k,\Delta,\zeta} \left[\sqrt{\Delta} f_k \zeta \right]}{\sqrt{q}} = -\frac{\alpha \mathbb{E}_{k,\Delta,\zeta} \left[\sqrt{\Delta} \partial_\zeta f_k \right]}{\sqrt{q}} = \alpha \mathbb{E}_{k,\Delta,\zeta} \left[\frac{\Delta \partial_\eta^2 \ell_k(\Delta v f_k + \omega_k)}{1 + v \Delta \partial_\eta^2 \ell_k(\Delta v f_k + \omega_k)} \right], \quad (71)$$

where $\partial_{\eta}^2 \ell_{\pm}(\eta) = [4(\cosh \eta/2)^2]^{-1}$ is the second derivative of the logistic loss. This equation is found to be much more stable.

Numerical experiments Numerical experiments regarding the quadratic loss with ridge regularisation were performed by computing the Moore-Penrose pseudoinverse solution. For the logistic loss, we used the `LogisticRegression` module from the `Scikit-learn` package [45].